UPPSALA
UNIVERSITET

Digital Comprehensive Summaries of Uppsala Dissertations from the Faculty of Pharmacy 295

Powder mechanics and dispersion properties of adhesive mixtures for dry powder inhalers

Conceptualized as a blend state model

JONAS RUDÉN

ACTA
UNIVERSITATIS
UPSALIENSIS
UPPSALA
2021

ISSN 1651-6192
ISBN 978-91-513-1167-8
urn:nbn:se:uu:diva-438081

Dissertation presented at Uppsala University to be publicly examined in Room A1:111, Biomedicinskt Centrum (BMC), Husargatan 3, Uppsala, Wednesday, 12 May 2021 at 10:15 for the degree of Doctor of Philosophy (Faculty of Pharmacy). The examination will be conducted in English. Faculty examiner: Professor Regina Scherliess (Institute of Pharmacy, Faculty of Mathematics and Natural Sciences, Kiel University).

Abstract
Rudén, J. 2021. Powder mechanics and dispersion properties of adhesive mixtures for dry powder inhalers. Conceptualized as a blend state model. *Digital Comprehensive Summaries of Uppsala Dissertations from the Faculty of Pharmacy* 295. 62 pp. Uppsala: Acta Universitatis Upsaliensis. ISBN 978-91-513-1167-8.

Inhaled medicines is a therapy that dates back several thousands of years. Nowadays, using various types of inhaler devices to deliver active pharmaceutical ingredients (APIs) to treat respiratory diseases has become common practice. One such device is the dry powder inhaler (DPI) which often contains an adhesive powder mixture consisting of micron-sized API particles and larger inert particles (carriers). The general goal of a DPI formulation is to reach as high inhalable dose (dispersibility) as possible while maintaining a low dose variability. In addition, the formulation has to be stable during manufacturing and handling to avoid segregation. In this thesis, critical properties of adhesive mixtures for DPIs have been identified and summarized in a blend state model that describes the spatial distribution of API- and carrier particles in a mixture. The model consists of four distinct states, which are identified using a combination of powder mechanical analysis and imaging techniques. In the first state, denoted S1, the drug deposits at the open pores of the carriers resulting in a denser powder packing but a low dispersibility. At the second state, S2a, the drug will adhere to the outer carrier surfaces, which results in a more porous powder packing and increased dispersibility. Following further increases in drug load, reaching the S2b state, the adhering drug layer grows in complexity resulting in further reductions in powder density but with additional increases in dispersibility. At the final state, S3, the mixture is oversaturated with fines, which results in segregation and large self-agglomerates that are poorly dispersed during an inhalation experiment. The evolution of the blend state was found to be dependent on the carrier and API properties such as size and shape. Irregular carriers could handle higher drug loads before segregation occurred, while irregular API particles formed more porous adhesion layers resulting in lower drug loads. In terms of dispersibility, it was found that porous adhesion layers were more easily dispersed than coherent adhesion layers. When varying the pressure drop (airflow rate), the dispersibility of the S1 state increased linearly with higher pressure drops. However, S2a-S3 were more or less insensitive to increased pressure drops above a certain critical pressure drop. With the blend state model and the mapping of the evolution in blend state with increased drugs loads, the formulation work can ideally be improved leading to more effective treatments for patients.

Keywords: Inhalation, Dry Powder Inhaler, adhesive mixture, aerosols, powder mechanics, dispersibility, aerosolization

Jonas Rudén, Department of Pharmaceutical Biosciences, Box 591, Uppsala University, SE-75124 Uppsala, Sweden.

ISSN 1651-6192
ISBN 978-91-513-1167-8
urn:nbn:se:uu:diva-438081 (http://urn.kb.se/resolve?urn=urn:nbn:se:uu:diva-438081)

Till mormor

“We don’t make mistakes, only happy little accidents.”
– Bob Ross

List of Papers

This thesis is based on the following papers, which are referred to in the text by their Roman numerals.

I. **Rudén, J.**, Frenning, G., Bramer, T., Thalberg, K., & Alderborn, G. (2018). Relationships between surface coverage ratio and powder mechanics of binary adhesive mixtures for dry powder inhalers. *International journal of pharmaceutics*, 541(1–2), 143–156.

II. **Rudén, J.**, Frenning, G., Bramer, T., Thalberg, K., An, J., & Alderborn, G. (2019). Linking carrier morphology to the powder mechanics of adhesive mixtures for dry powder inhalers via a blend-state model. *International journal of pharmaceutics*, 561, 148–160.

III. **Rudén, J.**, Frenning, G., Bramer, T., Thalberg, K., & Alderborn, G. (2020). On the relationship between blend state and dispersibility of adhesive mixtures containing active pharmaceutical ingredients. *International Journal of Pharmaceutics: X*, 3, 100069

IV. **Rudén, J.**, Frenning, G., Bramer, T., Thalberg, K., & Alderborn, G. (2020). Effect of pressure drop on blend state-dispersibility relationships of adhesive mixtures for inhalation. *(In manuscript)*

Contents

Abbreviations

AFM	Atomic Force Microscopy
API	Active Pharmaceutical Ingredient
BET	Brunaur Emmett Teller
CBD	Compressed Bulk Density
COPD	Chronic Obstructive Pulmonary Disease
DPI	Dry Powder Inhaler
ED	Emitted Dose
FPD	Fine Particle Dose
FPF	Fine Particle Fraction
FSI	Fast Screening Impactor
HR	Hausner Ratio
LABA	Long-Acting β_2 Agonist
MMAD	Mass Median Aerodynamic Diameter
MOC	Minimum Orifice diameter
NGI	Next Generation Impactor
OIP	Orally Inhaled Product
pMDI	pressurized Metered Dose Inhaler
SABA	Short-Acting β_2 Agonist
SCR	Surface Coverage Ratio
SEM	Scanning Electron Microscopy
UBD	Unsettled Bulk Density
UPLC	Ultra Performance Liquid Chromatography
WHO	World Health Organization

Introduction

Aerosols

The term *aerosol* was coined in 1932 and originates from the Greek word *aer* (air) and the Latin *sol* (solution) describing the entrainment of droplets in air (1). Nowadays, the term aerosol is used to describe both droplets and particles dispersed in a gaseous phase (2). In orally inhaled products (OIPs), both solid particles and liquid droplets are present (3). However, how the aerosols are generated differs depending on the type of inhaler device that is used. For nebulizers, aerosols are typically generated from a solution using a vibrating mesh or an oscillating membrane (4, 5). For pressurized metered dose inhalers (pMDI), the aerosols are typically generated from particles suspended in a propellant gas that quickly expands upon activation to generate a plume of particles (5, 6). In contrast to the other devices, dry powder inhalers (DPI) normally rely solely on the inspiratory airflow of the patient to aerosolize a powdered mixture containing *active pharmaceutical ingredients* (APIs) (7, 8).

Once emitted from the any of these types of inhalers, the aerosols will be inhaled by the patient. Where in the respiratory system the aerosols will deposit depends on the aerodynamic diameter of the aerosols and the lung (patho-)physiology of the patient (9, 10). The aerodynamic diameter is an equivalent diameter, meaning it is not a diameter of an actual particle, but instead the diameter of a sphere of unit density with the same settling velocity as the actual particle of interest (9, 11). The idea of using an aerodynamic diameter is to simplify the complexity of real particles that are polydisperse that is, particles that vary in both shape and size. Using the aerodynamic particle diameter also makes it possible to relate particle behavior in a pharmaceutical impactor (*in vitro*) to how the particles would behave *in vivo* (i.e., where in the respiratory system they would deposit) (12-14).

There are three major types of deposition mechanisms: diffusion, sedimentation, and inertial impaction (9, 15, 16). For particles with an aerodynamic particle size less than 0.5 μm, diffusion is the main mechanism. Particles in this size-range will be entrained in the air and move with Brownian motions until the particles meet a surface. Sedimentation is the main mechanism for particles from 0.5 to about 5 μm; these particles will sediment over time solely because of gravity. For particles in the range 5–10 μm, inertial impaction is the most prominent mechanism (9, 15). When emitted from the inhaler, the

particles will reach a certain initial velocity dependent on the inspiratory airflow of the patient (nebulizer/DPI) or the expansion of the propellant (pMDI). A higher initial velocity will make the particles more likely to impact because they will have increased momentum or inertia. Larger particles with a higher mass (more energy) are thus more likely to deviate from the direction of the airflow and impact than smaller particles (15).

As will be discussed in the next section, the airways of the human respiratory system continuously shrink in size starting from the oral cavity and progressing to the terminal bronchioles in the lower parts of the lung (17). Airflow is also significantly reduced between these stages (10), which means that in the larger airways, the particles are more likely to deposit due to inertial impaction, while in the smaller airways (bronchioles), sedimentation of particles is the most important mechanism. In the smallest region (alveolar), sedimentation and diffusion will occur because the airflow is practically zero (9, 10, 15). Thus, the smaller the aerodynamic particle diameter, the further the particles will go into the lungs. However, if the particles are not deposited, they will simply be exhaled.

Respiratory anatomy and physiology

The human respiratory system can be divided into two main regions: the *conducting zone* and the *respiratory zone*. The conducting zone includes the *nasal* and *oral cavities*, the *throat* (*pharynx*), the *bronchi*, the *bronchioles* and the *terminal bronchioles*. These anatomical regions are designed to guide the air towards the respiratory zone, where the gas exchange occurs, which includes the *respiratory bronchioles*, *alveolar ducts* and the *alveoli* (17, 18).

The main function of the respiratory system is to oxygenate the blood needed for cellular respiration. This occurs when the *diaphragm* contracts during breathing, expanding the lung, and the resulting air pressure drop, compared to atmospheric pressure, forces air into the lungs. However, many disease states will reduce the function of the respiratory apparatus, and thus, many OIPs are aimed at restoring normal lung function. In the following two sections, the anatomy and physiology of the respiratory system will be presented. In the third section, the pathophysiology (i.e. disease state) of common lung diseases will be discussed.

Conducting zone

A sketch of the conducting zone is presented in Figure 1. During inhalation, air travels through the nose/mouth, throat, trachea and all the way down to the alveoli, where gas exchange occurs (17). From the trachea, the airways are subsequently divided into smaller and smaller airways. In total, the conductive

airways have 16 subdivisions, where the smallest airways (terminal bronchioles) are less than 0.6 mm in diameter (19). The trachea and the larger bronchi have the same type of cellular structures with thicker mucosal epithelium containing ciliated cells (which function to remove foreign objects) and goblet cells that produce mucus (which provides additional protection to these cells) (17, 19). These airways are also supported by cartilage structures to provide strength and rigidity to the airways. Once the bronchioles are reached, the epithelium is significantly thinner and no mucus-producing cells are present (17, 20). In the bronchiole region, there is no cartilage to support the airways; instead, they have a complete layer of smooth muscle that controls the size of airways to regulate airflow (17). This control is accomplished through the innervation of *parasympathetic* (constriction) and *sympathetic* (dilation) nerve-endings. The primary receptor type for the sympathetic nerves in the lung is of the *β_2-type*, which is of relevance for selective drug development as will be discussed in the section *Therapeutic aerosols for inhalation.*

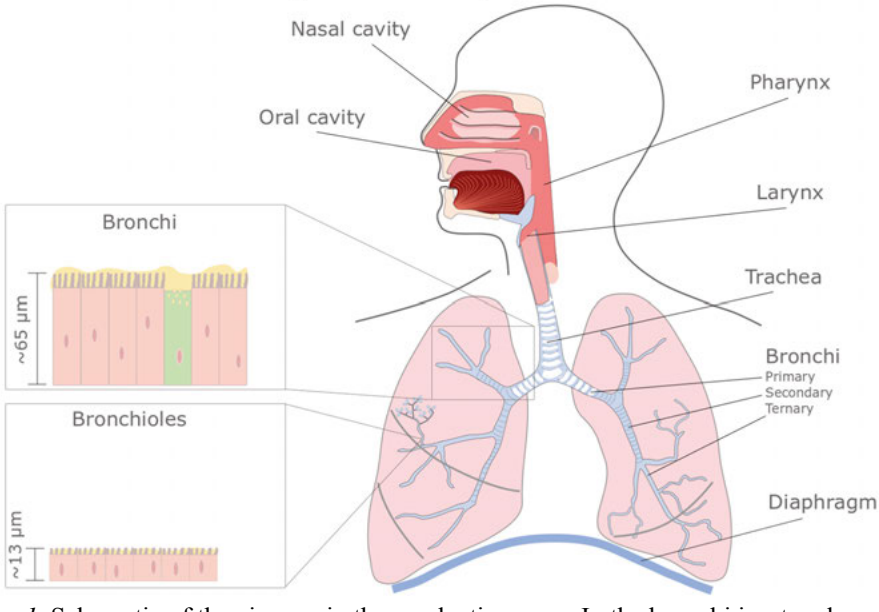

Figure 1. Schematic of the airways in the conducting zone. In the bronchi inset, yellow represents the mucus layer, while a goblet cell is indicated in green. Cilia-bearing epithelial cells are in pink in both insets.

Respiratory zone

In the respiratory zone (Figure 2), the airways continue to divide into smaller airways (divisions 17-23) (10). As the airways become smaller, the total cross-sectional area is increased as the airways increase in number (19). In the alveolar region, where there are estimated to be between 300–500 million alveoli (10, 17), the total surface area is around 100 m^2 (10, 19). This surface, together

with an extremely thin epithelium comprising mainly *Type I-cells* (0.1–0.2 µm) (19), provides excellent conditions for gas exchange. The large surface area of the lung together with a high throughput of blood also makes this system a promising route for systemic drug delivery (19, 20).

In the alveoli, there are no cilia to remove any foreign objects. Instead, the alveoli host macrophages that engulf and remove debris. There is no mucus, but instead a very thin layer of lung fluid excreted by the other major cell type in the alveoli, the *Type II-cells* (19). The main function of this fluid, which contains surfactants, is to reduce the surface tension to make for effortless breathing when the lung expands during inhalation (17).

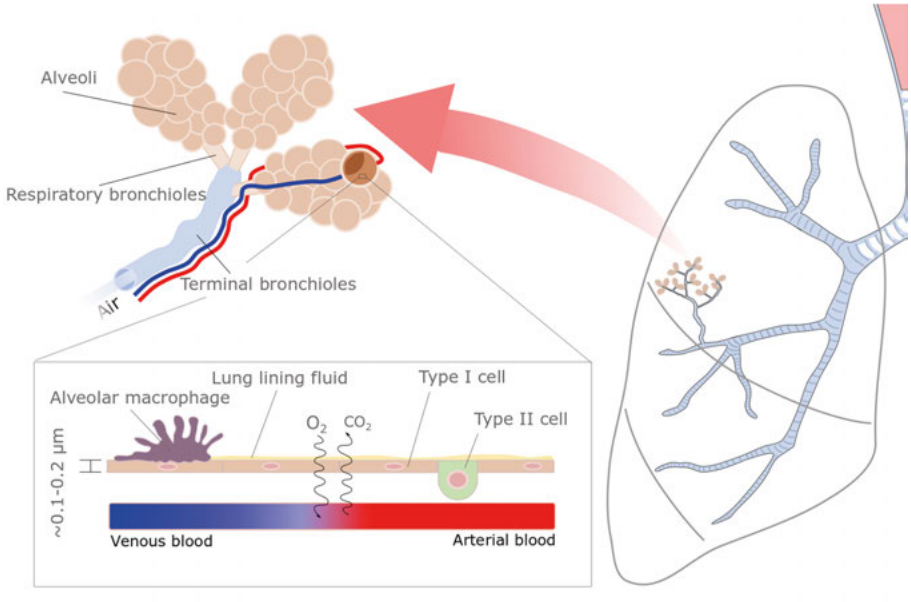

Figure 2. Schematic of the airways in the respiratory zone.

Pathophysiology

Lung diseases are among the most common medical conditions in our society today. According to the World Health Organization (WHO), there are around 339 million cases of *asthma* worldwide and 250 million cases of *chronic obstructive pulmonary disease (COPD)* (21, 22). COPD alone is the cause of millions of premature deaths each year and is expected to become the 3rd highest leading cause of death worldwide by 2030 (23). For these reasons, developing safe and effective OIPs to treat these two diseases is crucial.

Asthma

Asthma is characterized by an increased sensitivity to inhalation of various stimuli such as allergens, smoke, or chemicals and is manifested by the constriction of the airways (10). The causes are normally an underlying allergy or long-term exposure to the aforementioned stimulants. The symptoms are usually heavy coughing and wheezing noises while breathing, and shortness of breath (10, 24). During severe asthma attacks, the conditions rapidly worsen. The treatment of asthma often includes inhaling anti-inflammatory drugs, most often corticosteroids, which reduces the response of the immune system (25). In addition, bronchodilating drugs are used to act on sympathetic nerves and quickly relive the symptoms (26).

Chronic Obstructive Pulmonary Disease

The term COPD is commonly used to define patients who have emphysema and/or chronic bronchitis (10). This condition is characterized by inflammation in the small airways with excessive mucus production in the case of bronchitis or permanent damage to the alveoli and the respiratory airways in the case of emphysema (10). The symptoms of COPD are similar to asthma, but often include coughing up mucus. The symptoms are also chronic in nature, while asthma is typically acute (27). The causes for COPD are often related to smoking or repeated exposure to different air pollutants (10) and it is treated with similar kind of drugs as for asthma but for adapted chronic use (28, 29). COPD gradually worsens over time leading to reduced lung function. Eventually, doing even simple tasks will lead to a shortness of breath. Due to the reduced function of the lung, COPD patients often suffer further complications such as pneumonia, which may be fatal (30).

In addition to COPD and asthma, there are several other lung diseases that are currently treated with inhaled therapies, or that are being researched for such treatment (31, 32). One notable disease is *cystic fibrosis*, a genetic disorder that produces thick mucus often leading to bacterial infections in more severe cases (10, 33). These infections are often treated with large doses of inhaled antibiotics.

In the next section, the history of therapeutic aerosols will be presented along with some notable examples of important discoveries in treating respiratory disease.

Therapeutic aerosols for inhalation

The treatment of respiratory diseases with inhaled medicines is a therapy that dates back several thousands of years (34). Findings on old Egyptian papyrus scrolls from 1554 BCE describe inhaling *black henbane*, which contains alkaloids such as *atropine* (which inhibits parasympathetic nerves) (35, 36). Other ancient practices of inhaling various substances for the treatment of disease, or for recreational purposes, have been discovered in many other cultures as well. In South and Central America, the natives smoked tobacco as early as 2000 years ago (36), and in China, smoking opium dates back approximately to 1000 BCE (35). In India, the physicians Charaka and Sashruta described the oldest form of inhaled asthma treatment, which date back to around 600 BCE (35). In their writings, they described the use of an herbal species called *dhatūra* (*Datura stramonium*) that could be smoked to relieve the symptoms of asthma. This herb also contains the substance atropine.

Other forms of asthma treatment had been in used even earlier, although oral form. In China, the use of *ephedra* (or Ma Huang) dates back to around 1000 BC in the oldest known book on internal medicine written by Huang-Ti (3, 35, 36), and ephedra was also used during the Roman Empire to treat asthma. Ephedra was later found to contain the active substance *ephedrine* (sympathetic agonist) which remained relevant well into the 20th century as a treatment for respiratory disease (35).

In ancient Greece, Hippocrates (c. 460 – c. 377 BCE) described a device capable of generating vapors from boiling herbs and resins to be inhaled to treat various diseases (35, 36). Greek physicians further developed inhaled treatments in the first centuries CE, when Galen of Pergamo and Aretaeus of Cappadocia both advocated the use of various soil and herbal powders for inhalation.

Technologies for inhalation were no more advanced than smoking or boiling various herbs until the end of the 1700s and the advent of the industrial revolution, although smoking vapors remained a common method of delivering therapeutic aerosols throughout the 1800s (35). Towards the middle and end of the 19th century, several technical advances were made in the pursuit of delivering pharmaceutical aerosols with the introduction of nebulizers and dry powder inhalers (35). An noteworthy example is the first pressurized inhaler, which was invented by Jean Sales-Girons in Paris 1858 (36).

In the late 19th and early 20th century, important discoveries were made about the treatment of respiratory diseases. In 1860, Henry Hyde Salter published a systematic review of the treatment of asthma, in which he distinguished between depressants, stimulants and sedatives (36). In 1912, Ephraïm used *adrenaline* for the first time to treat severe acute asthma (1), which is a drug still used for this purpose today. These aerosols could be delivered by atomizers, which are small perfume-like bottles with a squeeze ball (1). Later, Tiffeneau studied the effects of cholinergic and adrenergic aerosols, and from

his observations, he invented one of the earliest systems of determining the lung capacity of patients with lung disease, measurements that are now known as the forced expiration volume (FEV) and vital capacity (VC) ratio (1). He also investigated the physics of aerosols together with Brun, and in their studies, they observed that to avoid deposition of aerosols in the upper respiratory tract (pharynx), the aerosols had to be smaller than 5 microns (1). This proved to be a very important observation, and this size cut-off is still used today to describe which aerosols will enter the lower respiratory tract.

From around the 1950s and onwards, a real breakthrough in aerosol delivery and technology was made. The first ultrasonic nebulizer was introduced, which used vibrating elements to generate aerosols from liquids (1). These nebulizers were quite large and expensive (which they still are to this day) and thus not very patient-friendly. The limited efficiency of the nebulizers lead to the invention of the first pressurized metered dose inhaler (pMDI) in 1956 by George Maison and Charles Thiel of Riker Laboratories (now known as 3M Pharmaceuticals) (34, 35). Within two years of development, they launched two inhalers, one containing *adrenaline* and one containing *isoproterenol* (non-selective β_2 agonist). These devices were initially a huge success, but the non-selective action and potential danger of isoproterenol (inducing tachycardia) that was discovered shortly after its introduction led to its disuse in favor of the more selective short-acting β_2 agonist (SABA) substance *salbutamol* (34, 35).

Around the same time, the first successful use of *cortisone* to treat asthma was reported (34). Initially, corticosteroids were given orally, but even in low doses, these can cause serious side effects (such as diabetes, hypertension, osteoporosis and obesity) after prolonged use (37). In the early 1970s, with the introduction of the inhaled corticosteroid *beclomethasone*, the effective treatment of chronic asthma took a big leap forward (34). Introducing these drugs into different types of inhalers for patient use has since revolutionized the treatment of asthma.

After the introduction of the inhaled corticosteroids, long-acting β_2 agonists (LABA) were developed, with *salmeterol* and *formoterol* being the first drugs to hit the market. Nowadays, the treatment of asthma often includes both corticosteroids and LABAs if a low dose corticosteroid is not enough to relieve the symptoms (34).

The history of therapeutic aerosols is long and exciting and has led to many important discoveries and innovations over the years. The next section, which is the main area of research of this thesis, will describe solid dosage forms emitted from dry powder inhalers.

The dry powder inhaler

The first known dry powder inhaler (DPI) was invented by Ira Warren in Boston in 1852 (35). However, it took close to a hundred more years before the first commercial dry powder inhaler device, the *Aerohaler*®, was launched in 1948 by Abbott (12). This inhaler device was made to deliver *penicillin* together with a bronchodilator (7). The use of a DPI instead of a nebulizer or pMDI has several advantages. A dry powder generally has a much higher chemical stability than a solution or a suspension (7, 8). In addition, the devices can be made cheaply, they can be small, and they require no active mechanism except the patient's own inspiratory flow to generate the aerosols (7, 38). Compared to the pMDI, it is possible to deliver much larger doses through a powdered formulation (12). The DPI is also considered by many to be easier to use (leading to fewer critical patient errors) and the propellant gas in the pMDIs are based on hydrofluoroalkanes, which are potent greenhouse gases and undesirable from an environmental point of view (39, 40). Despite the advantages of DPIs, the pMDI remains the most prescribed type of inhaler device in the world today for the treatment of obstructive airway diseases (41).

The dry powders used in DPIs are either *carrier-free* or *carrier-based* formulations (42). In carrier-free formulations, the drug content is high and exists either as porous agglomerates of micronized drug particles (e.g. in *Turbuhaler*®) or as porous single particles (e.g. *TOBI Podhaler*®) (42). In the carrier-based formulations, larger particles called *carriers* are mixed with micronized drug particles called *fines* to spontaneously form *adhesive units*, where the fine particles are attached to the surfaces of the carrier particles (Figure 3) (8, 43, 44). A mixture containing these adhesive units are called an *adhesive mixture*. The carrier-based formulations are the basis of this thesis and will be further discussed in the next section.

Carrier-based formulations

The typical carrier used in carrier-based formulations for OIPs are in the size range of 50–200 μm and are usually based on α-lactose monohydrate (43, 45, 46), although other sugars such as mannitol are also used (47-49). The use of carrier particles in dry powders for inhalation are mainly for pharmaceutical reasons, as these carriers do not exert any pharmacological effect. Their main purposes are: 1) to convey sufficient powder flowability to the formulation to ensure proper filling and dose accuracy of the inhaler; 2) to aide in the dispersion of API into inhalable aerosols upon inhalation; 3) to reduce the risk of particle segregation (8, 50, 51).

Upon mixing carrier particles with fine APIs in the < 5 μm range, the high adhesive nature of the fine particles (high interparticulate attraction forces) makes them spontaneously attach to the carrier particles upon mixing (52-55),

thus forming adhesive units (Figure 3). During the mixing stage, natural occurring agglomerates of APIs must be disintegrated into smaller clusters or primary particles in order for the fines to form an adhesive unit with the carrier (56-59). After a sufficiently homogenous mixture has been produced, the next step in the process is to fill the powder into the dosing unit of the inhaler, e.g. capsule, blister or a powder reservoir (50, 60). The final step is to aerosolize the powder, which occurs when a patient inhales from the DPI. At this crucial step, the inspiratory flow must produce enough dispersive forces in order to detach the fine APIs from the carrier surfaces and transfer them into the lung (61-63). The carrier particles, which are too large to be inhaled, will impact in the mouth or throat and be swallowed (12, 15).

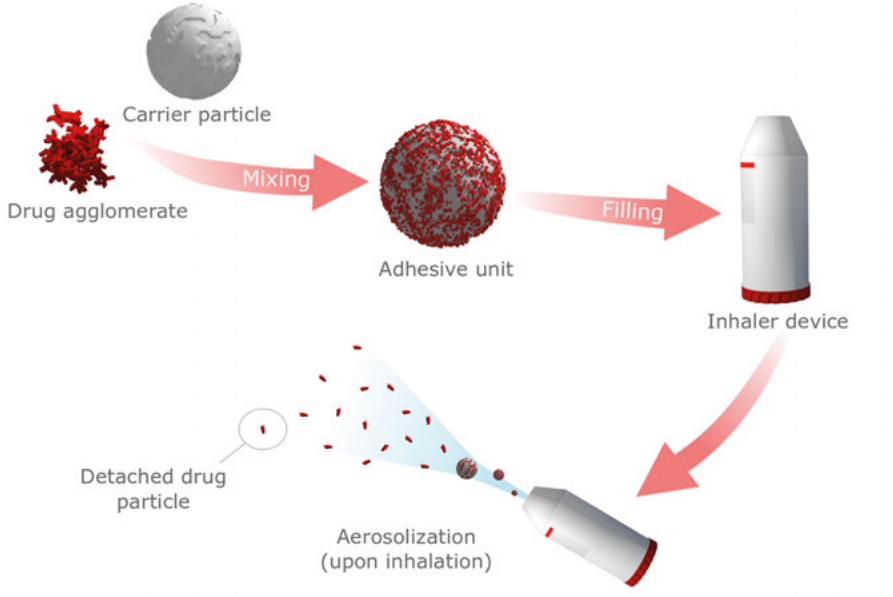

Figure 3. Carrier-based formulation, from formation to usage.

When formulating a carrier-based formulation, the end goal is to achieve the highest possible detachment efficiency (high dispersibility, which is a higher fraction of the total dose ending up in the lung) while keeping the formulation stable during manufacturing (64, 65). Several factors influence the dispersibility of the formulation, such as the size, shape and chemical properties of both the fines and carrier particles as well as the blending mechanisms and drug load (66-69). Each of these factors can ultimately affect the dispersibility in either a positive or a negative way depending on the interplay among them (43, 70). For instance, increased carrier surface roughness can be either beneficial or detrimental depending on the drug load and the API properties (71-74). To complicate matters further, the mixing time, mixing order and the type of mixer will also affect the dispersibility of the formulation (67, 75-77). On

the particle level, different attraction forces (i.e. surface energies) between carriers and fines are important (46, 62, 78, 79). If the attraction forces are too strong, the detachment of fines from the carriers will be low, but if they are too weak, the fine particles may segregate from the carriers during handling and use. During manufacturing, the risk of segregation is a common problem, and the variable forces induced during filling of the inhaler or capsule may affect the performance of the final product (50, 60, 80). In the context of filling, it is important that the flowability of the formulation is sufficient to minimize the risk of dose variability.

The individual particle properties of both fine drug and coarser carrier particles, combined with a set mixing condition, will result in a unique mixture structure (81). This structure will ultimately affect the dispersibility of the final formulation, but also the manufacturability, in that changes in powder flowability are dependent on this structure. In addition to the mixture structure (described in detail in the next section), knowing the type of inhaler device and a patient's inherent capability to produce a certain airflow (or create air pressure drop) are important for getting a properly dispersed and aerosolized powder (82). Typically, a pressure drop of 4 kPa is used for inhaler testing of DPIs. However, patients with a lung disease may not be able to achieve 4 kPa pressure drop through an inhaler device due to reduced lung capacity (83).

The mixture structure

The spatial distribution of fine drug and carrier particles in an adhesive mixture that is created upon blending will result in a certain mixture structure. What that mixture structure will look like, and how it will behave, will depend on particle properties such as size, surface energy, morphology, but perhaps more importantly, the drug load (81). A study by Young et al. (81) introduced the concept of the mixture structure, or formulation structure. The formulation structure could be divided into five stages depending on the drug load. In the first stage, the fine particles would adhere to 'high adhesion sites' and would thus be hard to disperse. In the next three stages, the dispersibility will increase following further additions of fines resulting in a growing adhesion layer. In the final stage, the carriers are vastly oversaturated and the dispersibility is reduced while segregation is increased. In a later study by Hertel et al. (84), similar mechanisms explaining the dispersibility were discussed. The study involved the use of carriers of varying complexity (i.e. size and shape) with increased drug loads, and touched on the effect of higher drug loads on the flowability of adhesive mixtures. In a mechanistic study about the bulk and tap densities of binary mixtures, a hypothetical mixture structure was constructed using two spherical entities (85). The authors theorized that an optimal packing structure of two particle types of significant size differences could be achieved.

From these studies, it can be concluded that the resulting mixture structure of a certain combination of carriers and fines is an important property governing the performance of adhesive mixtures, from both the dispersibility and manufacturability aspects. The term *powder mechanic*s can best be described as the packing and flow of particulate solids (86). Knowing this kind of information about the formulation has historically been important for the manufacturability of various powders (50, 85). However, this knowledge has also been shown to be useful in the prediction of device filling and dispersibility of adhesive mixtures (84, 87-89). The link between the powder mechanics and the performance of carrier-based mixtures is thus obvious, and hence, studying the powder mechanics could potentially be useful to assess the mixture structure.

Aims of the thesis

The overall aim of the thesis project was to derive new knowledge about critical powder properties of adhesive mixtures that can be promptly implemented as improved strategies and technologies for the formulation of dry powder inhalers. With this in mind, the specific aim was to expand on the mixture structure concept, with the use of extensive powder mechanical analysis and visualization techniques, and to develop a model to explain the behaviour of adhesive mixtures in a simple way. The experiments conducted in this thesis can be divided into two main parts, the first concerning powder mechanics, and the second concerning dispersibility. The first two papers were focused on understanding the powder mechanics of adhesive mixtures with varying drug loads and with carriers of different complexities. The last two papers focused on expanding on the *blend state model* developed in the first part, and using this concept to study and explain the dispersibility of adhesive mixtures existing in the defined states of the model.

The specific aims of the papers comprising this thesis are:

I To study the relationship between the content of fine particles (expressed as a surface coverage ratio) and the observed powder mechanics of binary adhesive mixtures, and link these observations to the blend state of the mixtures.

II To investigate how carrier morphology affects the expression of blend states in adhesive mixtures, and at which surface coverage ratios transitions between states occur.

III To study the effects of different fines on the evolution of the blend state, and to investigate the dispersibility of each blend state in order to determine the relationship between blend state and blend dispersibility.

IV To investigate the effect of varied pressure drops on the blend state – blend dispersibility relationships, and to evaluate the usefulness of dispersion profiles for characterizing adhesive mixtures.

Methods

Materials

Selection of fine and carrier materials

Carrier particles based on α-lactose monohydrate were used in all studies in this thesis. In **Papers I–IV**, spray-dried carrier material called Lactopress SD was used. In **Paper II**, four additional carriers of inhalation grade were used with varying sizes, shapes and surface irregularities. The fine material (i.e. particles < 5 μm) used in **Papers I–II** was micronized lactose fines. In **Paper III**, the fine materials were the active pharmaceutical ingredients *budesonide*, *salbutamol* and *AZD5423*, each of which had been micronized into sizes suitable for inhalation. The first two compounds are widely used model compounds. In **Paper IV**, fines of budesonide were primarily used, in addition to the lactose fines from previous papers.

Particle characteristics

In order to understand the behaviour of powdered materials, the particle properties, such as size, density, and surface area, need to be characterized. The methods used are briefly described in the two following sections.

Particle size and density

The particle size of the fine and carrier materials was determined using laser diffraction (**Papers I–III**). The equipment used was a Sympatec HELOS particle sizer with a RODOS dispersion unit (Sympatec GmBH, Clausthal-Zellerfield, Germany). Different lenses were applied depending on the particle size of the material. The dispersion pressure used was 4 bar for all materials. From the volume distribution, the median particle size (D_{50}) as well as the relative width of the distribution (span) was calculated. The span was calculated using equation 1, where D_{90} and D_{10} are the diameters at the 90^{th} and 10^{th} percentiles of the volume distribution, respectively.

$$\text{Span} = \frac{D_{90} - D_{10}}{D_{50}} \quad (1)$$

The particle density, which was used for the calculations of surface area in **Paper I–III** (see next section), was assessed using helium pycnometry (Accupyc 1330, Micromeritics Instruments, Norcross, USA).

Surface area

In this thesis, two different types of surface areas were obtained, called *permeametry* and *gas adsorption* surface areas. The permeametry surface area was measured using either a Blaine apparatus (transient permeameter) (**Papers I–III**) or a steady-state permeameter (**Papers I–II**). The Blaine apparatus was used to measure the surface area of the fine particles, while the steady-state permeameter was used for the larger carrier particles. The permeametry surface areas were calculated using the Kozeny-Karman equation (90, 91). For the fine particles, a slip-flow correction was made in order to compensate for the passage of air along the walls of the container. The permeametry surface areas were used in this thesis to calculate the *surface coverage ratio* (SCR), i.e. the fines-to-carrier ratio required to theoretically cover a certain surface of a carrier particle with fines (see next section).

The gas adsorption surface area was assessed using a Tristar III 3020 (Micromeritics Instruments, Norcross, USA) instrument (**Papers II–III**). The adsorption gas was nitrogen, and the calculation of the surface area was done using Brunaur Emmett Teller (BET) theory from the obtained isotherms (92). The calculations were based on 6 data points in the 0.05 to 0.35 relative pressure range.

Preparation of adhesive mixtures

To determine the drug load of the adhesive mixtures, the fines-to-carrier ratio required to reach a certain *surface coverage ratio* (SCR) was calculated. The SCR approach was used in all studies in this thesis to determine the drug load of the mixtures and was thus a central part of this work. SCR was calculated using the following equation 2 (**Paper I**):

$$\text{SCR} = \frac{\alpha\, m_{\text{f}}\, S_{w,\text{f}}}{m_{\text{c}}\, S_{w,\text{c}}} \quad (2)$$

where m_f and m_c are the mass of fines and carrier material, while $S_{w,f}$ and $S_{w,c}$ are their mass specific surface areas (obtained from permeametry). The factor α is obtained from the ratio between the projected and total areas of a sphere and set to $1/\pi$. This factor is adapted from Dickhoff et al. (66) and is based on the fact that spherical particles in close packing are unable to completely cover a surface without overlapping, and they assumed that a spherical particle occupies an area equal to the square of its diameter (illustrated in Figure 4). In reality, this is a simplification, as fine particles can assume practically any shape. To clarify the meaning of the SCR, a surface coverage ratio of 1 would mean that the available carrier surface is completely covered with fines (i.e. 100% coverage). Thus, a value above unity would mean that multilayers of fines are theoretically formed on the carrier surface.

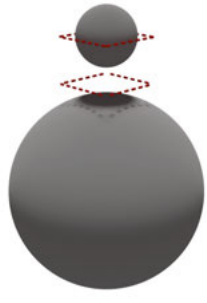

Figure 4. Illustration of the adhesion of a spherical fine particle on a spherical carrier particle as a projected square of its diameter.

The different mixtures made in this thesis had SCRs between 0.25 and 6. All binary mixtures were made in a similar manner, where the fines were sandwiched between the carrier material (corresponding to the target SCR) in a glass container. A fill volume of 50% was used as calculated based on the materials' respective bulk densities. Mixing was then done using a Turbula T2F (Willy A. Bachofen AG, Switzerland) low-shear blender operated at 46 rpm for 1 hr (Figure 5). For the ternary mixture used in **Paper IV**, two additions of fines were made with a mixing step after each addition.

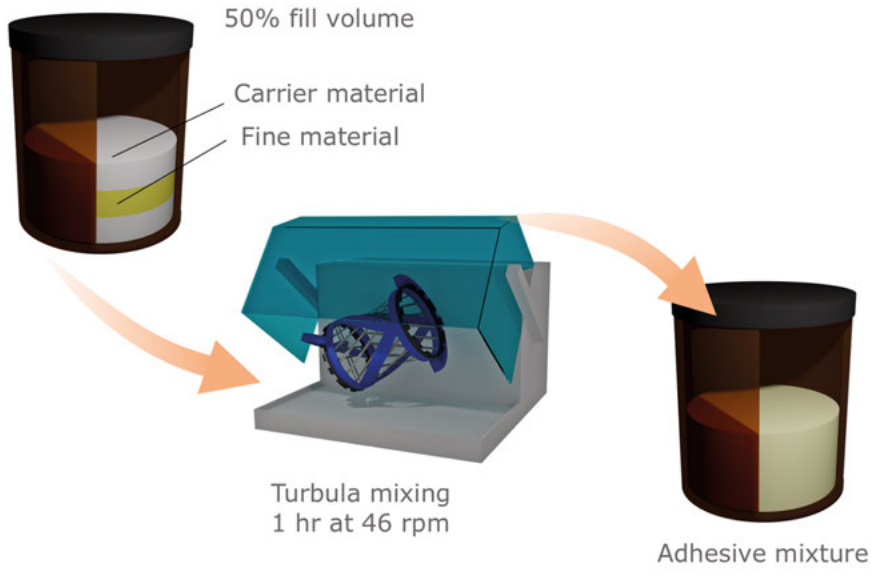

Figure 5. The mixing procedure.

Particle and adhesive mixture morphology

The shape of the individual particles as well as the appearance of the mixtures were studied using a number of different techniques with different uses dependent on what information was needed. The different techniques used in this thesis are explained in the next four sections.

Scanning electron microscopy

In order to get high resolution and detailed information about particle morphology, and the shape and general appearance of the adhesive units, scanning electron microscopy (SEM) was used in all papers of this thesis. SEM samples were generally prepared by sprinkling either raw material or adhesive mixture over a carbon tape followed by gentle tapping to remove excess material. The samples were then coated with platina/gold to minimize charging effects. The adhesive mixtures were observed using a Hitachi TM3030 Plus microscope (Hitachi, Tokyo, Japan) while the raw materials were studied using a Zeiss 1530 microscope (Carl Zeiss, Oberkochen, Germany). Pictures of the materials and mixtures were taken using a magnification ranging from 100–10,000x.

Light microscopy

In the mixtures with higher concentrations of fines, larger *self-agglomerates* formed were studied using light microscopy instead of SEM. In **Paper II** and **III**, the adhesive mixtures containing self-agglomerates were sprinkled over a petri dish and studied using a Zeiss Stereo microscope (Carl Zeiss, Oberkochen, Germany). Images were taken at 1x magnification.

QicPic

As a complement to the microscopy techniques and a way to achieve quantitative data of the shapes of the carrier particles, a high-speed imaging instrument QicPic (Sympatec GmBH, Clausthal-Zellerfield, Germany) equipped with a gravimetric feeding system was used (**Paper II**). During a measurement, images of the particles passing through the sensing zone were captured. The projected area diameter was calculated for each particle resulting in a diameter distribution. A series of Feret diameters (93) were also determined for each particle in 0° to 180° orientations. From these Feret diameters, an aspect ratio (AR) was calculated according to equation 3 using the maximum (F_{max}) and minimum (F_{min}) Feret diameters for each particle.

$$\mathrm{AR} = \frac{F_{\max}}{F_{min}} \tag{3}$$

Atomic force microscopy

As a complement to the SEM images and as a way to get high-resolution topography data, an atomic force microscopy (AFM) instrument was used to study the carrier particles in **Paper II**. The instrument used was an Icon AFM (Bruker, NanoScope V controller, Santa Barbara, California, USA) in the tapping mode in air. Due to the size and morphology of the carriers, the cantilever tip lost contact with the surface when the scan area exceeded 20x20 µm for most carriers. In order to get comparable images, a scan area of 20x20 µm, corresponding to 256×256 pixels per scan, and a constant scan rate of 0.5 Hz was used for all carrier samples.

Mixture homogeneity

The mixture homogeneity was assessed using either laser diffraction or ultra-performance liquid chromatography (UPLC). For the pure lactose blends, the homogeneity was estimated by laser diffraction through the dry dispersion of approximately 500 mg of adhesive mixture at a pressure of 4 bar (**Papers I–II**). The < 5 µm content of the particle size distribution was then compared among the samples. For each blend, 10 samples were analysed.

To determine the mixture homogeneity of the drug-containing mixtures, UPLC-UV analysis was performed (**Papers III–IV**). Mixture samples were drawn from selected adhesive mixtures and the content of API in the samples was subsequently determined. A Waters Acquity UPLC system (Waters Corp, Milford, USA) equipped with a C18 BEH 1.7 µm 2.1x50 mm column and a photo diode array (PDA) detector was used to analyse the API content both for the homogeneity analysis as well as for the dispersibility assessment (see next section, *Dispersibility*).

Powder mechanics

The powder mechanics, i.e. the packing and flow of particulate solids, can be assessed using many techniques (94). The different methods used in this thesis will be explained in the following subsections. Figure 6 is an illustration of the different instruments used.

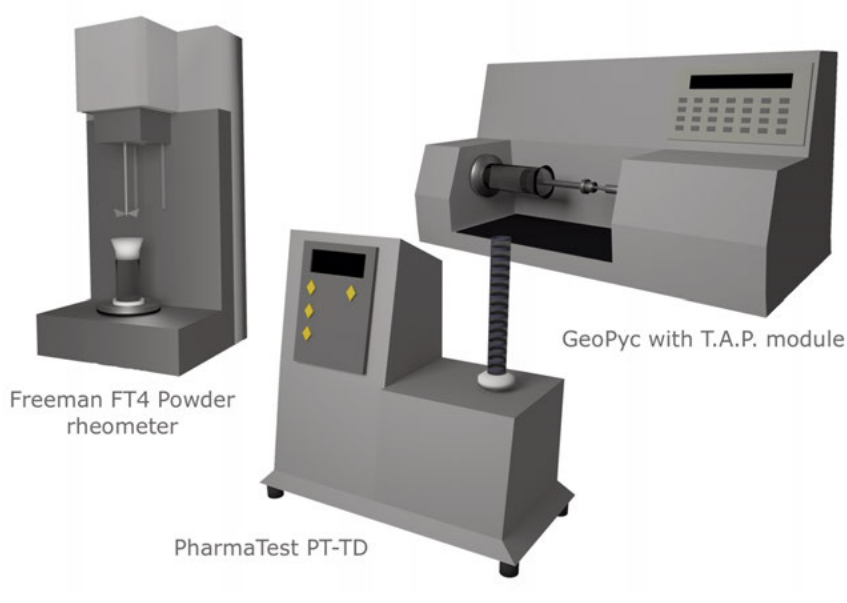

Figure 6. The Freeman FT4 Powder rheometer, the GeoPyc, and the PharmaTest PT-TD instruments used to assess the powder mechanics.

Unsettled bulk density

The unsettled bulk density (UBD) was measured using three different techniques in **Paper I** and one technique in **Papers II–IV**. The term 'unsettled' indicates that no force of consolidation other than gravitational force was applied during testing of the powder. The first unsettled bulk density (UBD_{AZ}), which was used in all papers, was determined using a steel cylinder with a well-defined volume (20.05 ml) manufactured by AstraZeneca R&D (Gothenburg, Sweden). During the filling of the sample cylinder, a taller hollow cylinder was filled with powder. The hollow cylinder was then lifted, filling the sample cylinder, and excessive powder was gently scraped off. The sample cylinder was weighed before and after filling, and a bulk density could thus be calculated. The second unsettled bulk density (UBD_{FT4}) was measured using the Freeman FT4 Powder Rheometer (Freeman Technology, Tewkesbury, UK), which gently mixes the sample with a steel blade before calculating the bulk density. The third unsettled bulk density (UBD_{Glass}) was measured using a 50 ml glass cylinder after filling with consecutive powder additions (using a spoon) until 20–25 ml of the cylinder was filled with powder. Reported bulk density values are the mean of three measurements.

Compressed bulk density

The compressed bulk density (CBD) was determined using three different procedures to consolidate the powders. All three techniques were used in **Paper I**. CBD_{Glass} was determined using the same cylinder as for the UBD_{Glass} and a PharmaTest PT-TD (Pharma Test Apparatebau AG, Hainburg, Germany) tapping instrument. The CBD_{Geopyc} was determined as described by Thalberg et al. (50) using a GeoPyc with the T.A.P. module (Micrometrics Instruments, Norcross, USA). A sample cylinder was filled with a few grams of powder and mounted horizontally to the instrument. During the test, the sample cylinder was rotated in an oscillating motion while compressing the sample with a force corresponding to a pressure of 35 kPa. Finally, the CBD_{FT4} was calculated after compressing the powder at normal stresses ranging from 1–30 kPa using the FT4 Powder Rheometer (see next section. *Powder rheometry*). Combining the UBDs and CBDs from the different techniques, three different Hausner ratios (HR) could be calculated (Eq 4). This last technique was also used in **Papers II–III** to study the compressibility and calculate the Hausner ratio. In equation 4, the *x* indicates each of the various techniques.

$$\mathrm{HR} = \frac{CBD_x}{UBD_x} \tag{4}$$

Powder rheometry

A tool that has been gaining in popularity in recent years for studying powder mechanics is the Freeman FT4 powder rheometer (95). The instrument is versatile and the different methods used in this thesis will be described briefly in this section and in Figure 7 (additional in-depth theory behind the permeability, flowability energy and shear tests can be found elsewhere in the literature (95-97)). For the shear and permeability tests, a 25 mm (cross-section) borosilicate cylinder with a sample volume of 10 ml was used. For the flowability energy test, or dynamic test, a taller sample cylinder of 25 ml was used.

Permeability

During the permeability tests (**Papers I–III**), the powder sample was compressed with a normal stress (σ) ranging from 1–30 kPa using a ventilated steel piston and a perforated metal base-plate. During each test, air was forced through the powder bed from beneath at a constant rate of 2 mm/s. The air pressure drop was then recorded at increasing normal stresses. From the air pressure drop measured in the test, specific surface areas were calculated for the mixtures in **Paper I** using the same theory as with the permeametry surface areas, as previously described (see previous section *Surface area*). The compression procedure used in the test was used in the calculation of CBD_{FT4}, and thus to calculate the HR.

Cohesion

The shear test (**Paper I**) involved the use of a shear-head, which is a piston with several blades attached to it. During the shear test, the shear-head was lowered into the powder and a pre-defined normal stress (σ) of 4 kPa (called pre-consolidation stress) was applied. Following this stress, the shear-head was rotated at a constant rate (pre-shear) applying a shear stress (τ) to the powder until the steady-state flow was achieved. Subsequently, the sample was sheared to failure (incipient flow) at defined normal stresses below the pre-consolidation stress (1–3 kPa), generating a shear-point at each tested normal stress. A straight line was drawn through each shear point to generate the yield locus (97, 98). The shear stress is normally on the y-axis, while the normal stress is on the x-axis in a yield locus plot.

The cohesion (τ_c) value was extracted from the point where the yield locus crosses the y-axis. The cohesion thus represents the shear stress required to shear the powder at zero applied normal stress.

Flowability energy

For the flowability energy test (**Paper I**), prior to testing, the sample cylinder was filled with 15 ml of powder. The flowability energy test uses a rotating steel blade to displace the powder within the cylinder in consecutive downwards and upwards motions. The downwards rotational motion was kept at a blade tip speed of 100 mm/s for the first to the seventh consecutive measurements. For the 7th to 11th measurements, the rotational speed was gradually lowered from 100 to 10 mm/s. The upwards motion was kept constant throughout the test (40 mm/s). The test generates three parameters, two of which were used in **Paper I**. The first parameter is the Normalized Basic flowability energy (NBFE, mJ/g), which is the flow energy registered during the 7th downward rotational movement divided by the sample weight (96). The second parameter is the Specific Energy (SE), which is the mean energy registered during the 6th and 7th upward rotational movements of the blade at the same blade tip speed, divided by the sample weight. Because of the rotational direction of the blade and its inclined surface, the blade compresses the powder during its downward motion and lifts the powder during its upward motion. Hence, downward motion corresponds to a forced (or confined) flow, whereas the upward motion corresponds to an unconfined flow.

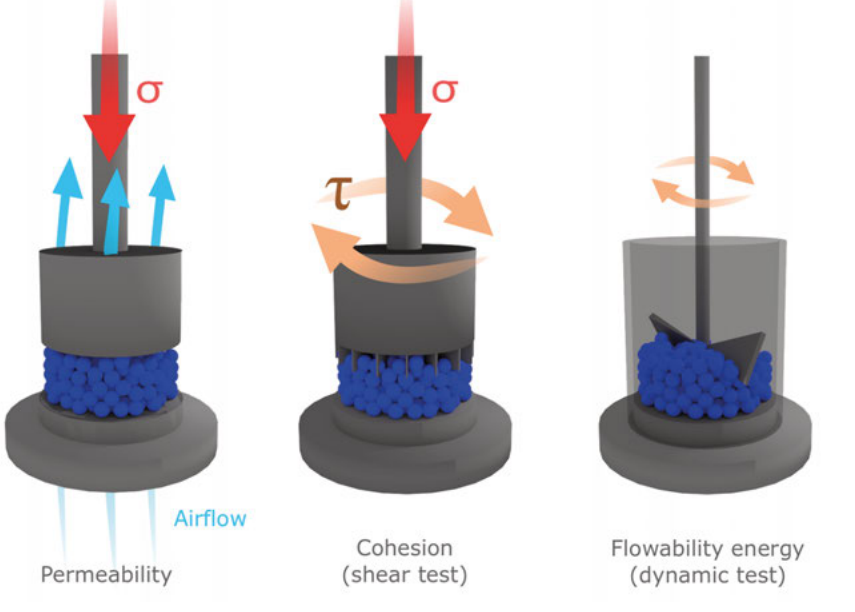

Figure 7. Illustration of the permeability, cohesion and flowability energy tests used with the FT4 Powder rheometer. The sigma (σ) indicates the normal pressure applied, while the tau (τ) indicates the shear stress.

Dispersibility

The dispersibility of the drug-containing mixtures used in **Papers III–IV** were assessed using either a *Fast Screening Impactor* (FSI) (Copley Scientific, UK) or a *Next Generation Impactor* (NGI) (Copley Scientific, UK). Regardless of the impactor used, the dispersion experiments were performed at ambient conditions, i.e. room temperature and ~30-45% RH. The Triggbox model III from FIA AB (Lund, Sweden) was the device used to measure the pressure drop, control the flowrate, and set the suction time in both studies.

Fast screening impactor

The dispersibility was assessed in **Paper III** using a FSI and a low resistance ScreenHaler device (99) (Figure 8). The airflow rate was set to 60 ± 0.3 L/min and the suction time to 4 seconds (corresponding to 4 L total suction volume). The drug content recovered from each stage of the impactor was quantified using the same UPLC system as described earlier (see previous section *Mixture homogeneity*).

Prior to testing, the inhaler device was manually filled with a dose varying from 15.0–17.5 mg for each single dispersibility test. For the mixtures with the lowest concentrations of API, 2 or 3 dose withdrawals were used in order to reach quantifiable amounts in the chemical analysis. The amount of API was determined at all three stages of the impactor, i.e. throat, pre-separator and filter. The samples were collected from each of these stages by first adding an internal standard solution or a specific amount of solvent (20 ml). Following this step, the throat and pre-separator were set to rotate using a Sample Preparation Unit (Copley Scientific, UK) for 20 min, while the filter was transferred to a petri-dish and set to shake on a shaking table for the same duration. After the sample preparation was completed, 0.5 ml from each stage was transferred into separate LC-vials for analysis. In the case of budesonide, 0.8 ml of phosphate buffer solution (pH 3.2) was added to the LC vials before the analysis.

For salbutamol and budesonide, the mobile phases were water and acetonitrile, both with 0.03% TFA. For AZD5423, the mobile phases were MilliQ water with 0.06% orthophosphoric acid and LC grade methanol. The salbutamol sample preparation involved only the addition of water, which is why no internal standard was used. For budesonide and AZD5423, the solutions included ethanol and thus internal standards were used to avoid the influence of significant evaporation. The internal standards used were fluocinolone acetonide for budesonide and 4-propyl hydroxy benzoate for AZD5423 (concentrations approximately 20 mg/L). The UV wavelength was set to 219 nm for salbutamol and 254 nm for both budesonide and AZD5423.

The amount of API in each stage was quantified from the response factors or area under the curve using calibration curves in the concentration range. The fine particle fraction (FPF, %) was then calculated as follows (Eq 5):

$$FPF = \frac{FPD}{ED} \times 100 \quad (5)$$

where the FPD represents the amount of drug (µg) deposited on the filter (aerodynamic cut-off of 5 µm) and ED (emitted dose) is the sum of drug (µg) on all three stages of the impactor.

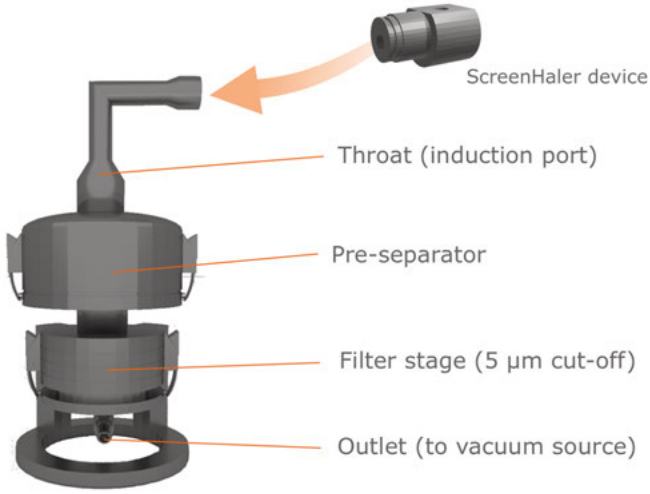

Figure 8. The Fast Screening Impactor (FSI) and ScreenHaler. During an experiment, the ScreenHaler is attached to the throat (or induction port) via an adapter. The function of the pre-separator is to collect larger particles (i.e. carrier particles). With the FSI setup, the pre-separator also blocks particles with an aerodynamic diameter > 5 µm.

Next generation impactor

To assess the dispersibility in **Paper IV**, a NGI was used together with a ScreenHaler device coupled with a *Turbuhaler*® mouthpiece (99) (Figure 9). The rate of airflow during measurement was set to match a pressure drop of 0.5, 2 and 4 kPa, and the suction time was adjusted to correspond to a total suction volume of 4 L. Before each dispersibility experiment, the NGI cups were coated with a solution of ethanol (51%), Brij 35 (15%) and glycerol (34%) (49) to reduce the risk of particle bounce between stages.

Prior to testing, the inhaler device was manually filled with a dose varying from 15.0–7.0 mg for each single dispersion experiment. Several dose withdrawals were used in order to reach quantifiable amounts in the chemical analysis (target emitted doses (ED) of around 3.2 mg were used). The emitted dose

was defined as the sum of masses of API collected in the throat, pre-separator and from largest to smallest diameter cut-offs of the impactor (stage 1 to MOC). Samples were collected from each stage by first adding 20 ml of an internal standard solution. Following this step, the throat and pre-separator were set to rotate using the sample preparation unit for 20 min, while the NGI cups were placed on a shaking table for the same duration. After the sample preparation was completed, 0.5 ml from each stage was transferred into separate LC-vials. The same UPLC analysis conditions were used as previously described for budesonide (see previous section).

The amount of API at each stage was quantified from the response factors using calibration curves in the concentration range. The mass median aerodynamic diameter (MMAD) was calculated for every dispersion experiment using Microsoft Excel 2016 (Microsoft, Redmond, USA) as instructed by the European Pharmacopoeia v9.0 (100). In short, the logarithmic values of the cut-off diameters at the specific flow rate were plotted against the inversed normally distributed values of the cumulative mass fractions (the "norm.inv" function in Excel). The resulting straight line was used to calculate the MMAD. Using the same calculations, the fine particle dose (FPD, in µg), which is the total mass of particles < 5 µm (i.e. LN(5)), was determined. The fine particle fraction (FPF, %) was then calculated using equation 5, but in this case, the ED was the total mass from throat to MOC.

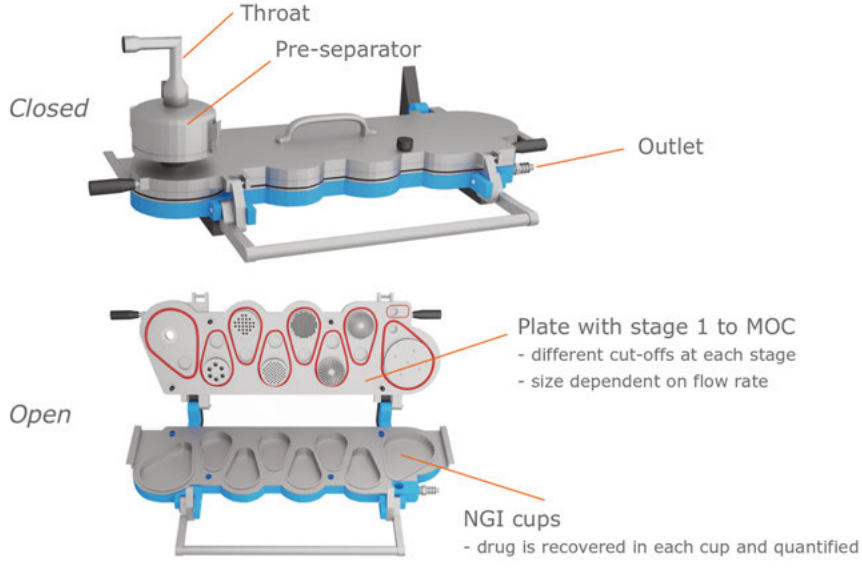

Figure 9: The Next Generation Impactor (NGI) in closed and open positions. The top plate includes smaller and smaller orifices from stage 1 to minimum orifice (MOC) that determines the aerodynamic size cut-off at each stage. This cut-off is dependent on the flowrate. The particles deposited at each stage are recovered and quantified post-impaction.

Results and discussion

The results and main findings from all four papers will be summarized in this section. For further details and a more comprehensive discussion, the reader is referred to each individual paper.

Particle properties

The particle and powder properties of all materials used in this thesis are summarized in Table 1. In the first two papers, only carrier particles and lactose fines were used. In the third and fourth paper, the Lactopress SD carrier was used together with the APIs.

Table 1. *Particle and powder properties of all materials. Average values with standard deviations in brackets (n=3).*

Material	SSA*, perm (cm^2/g)	SSA, BET (cm^2/g)	Particle size, D_{50} (μm)	Span	Bulk density (g/cm^3)
Respitose SV010	712 (13.1)	1682	106 (0.17)	1.13	0.70 (0.00)
Inhalac 230	778 (4.69)	924	131 (4.64)	0.88	0.70 (0.00)
Lactopress SD	778 (10.3)	1905	110 (0.55)	1.21	0.62 (0.00)
Respitose SV 001	332 (0.81)	874	213 (2.35)	0.76	0.72 (0.00)
Inhalac 70	300 (1.13)	872	213 (2.18)	0.76	0.64 (0.00)
Lactose fines	33134 (1933)	33427	2.70 (0.04)	2.16	0.23 (0.01)
Budesonide	50636 (2093)	56045	1.62 (0.02)	2.06	0.16 (0.00)
Salbutamol	59323 (280)	47323	1.87 (0.02)	2.03	0.12 (0.00)
AZD5423	36572 (809)	161465	1.80 (0.01)	2.15	0.18 (0.00)

*SSA = specific surface area

Carrier properties

In Table 1, the carriers can be grouped with respect to their median particle diameter into two groups with three materials of roughly 100 µm in diameter (Lactopress, Respitose SV 010 and Inhalac 230) and two of roughly 200 µm in diameter (Respitose SV 001 and Inhalac 70). For the permeametry-specific surface areas, the median particle diameters correlated inversely with the specific surface areas. For the carriers, the BET surface area was markedly higher than the permeametry surface area for four of the carriers, while for Inhalac 230, a more modest difference between the two types of surface areas was obtained. The type of surface area obtained from the permeameter can be regarded as an enveloped surface area (101), while the gas adsorption penetrates into the pores of particles, and thus, the area obtained using gas adsorption is increased for irregular particles (102). The relative width of the diameter distributions, expressed as the span, was generally higher for smaller sized carriers. Among the smaller carriers, Inhalac 230 had a narrower size distribution than both Lactopress SD and Respitose SV 010.

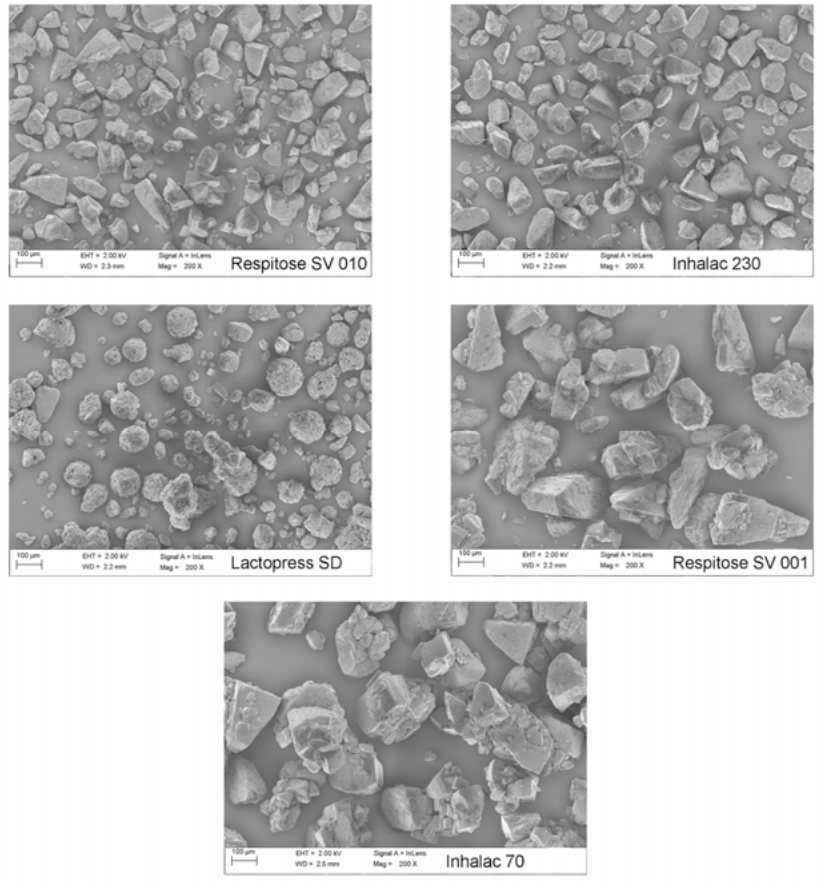

Figure 10. SEM images of the carrier particles taken at 200x magnification.

The size differences among the carriers noted in Table 1 can visually be observed (Figure 10), and the SEM images show that the Lactopress particles were the least elongated compared to the other particles, i.e. these particles can be described as nearly spherical but with a rough surface texture. The shapes of the other carriers, except Inhalac 70, were similar and can be described as "tomahawk shaped" particles, which is a term often used in the literature to describe the shape of lactose crystals. Inhalac 70, was a highly agglomerated carrier with a complex morphology with rougher surface texture.

Fine particle properties

The fines particles had a median particle diameter between 1.62–2.7 µm with a relatively high diameter span (Table 1). Like for the carrier particles, differences in fines particle morphology can also be observed (Figure 11). The SSA permeametry surface area was similar to the BET surface area, except in the case of AZD5423, which had observable nano-sized pores on its surfaces, contributing to a much larger BET SSA. The primary micro-particles of budesonide seemed relatively regular in geometrical shape with smooth surfaces, although some particles appeared to be significantly smaller than the median particle diameter, which could be the reason that budesonide had the lowest D_{50}. Particles of salbutamol and AZD5423 were irregular in geometrical shape, with observable elongated rod shaped particles. Some of the particles appeared to be larger than the D_{50} of 1.8 µm.

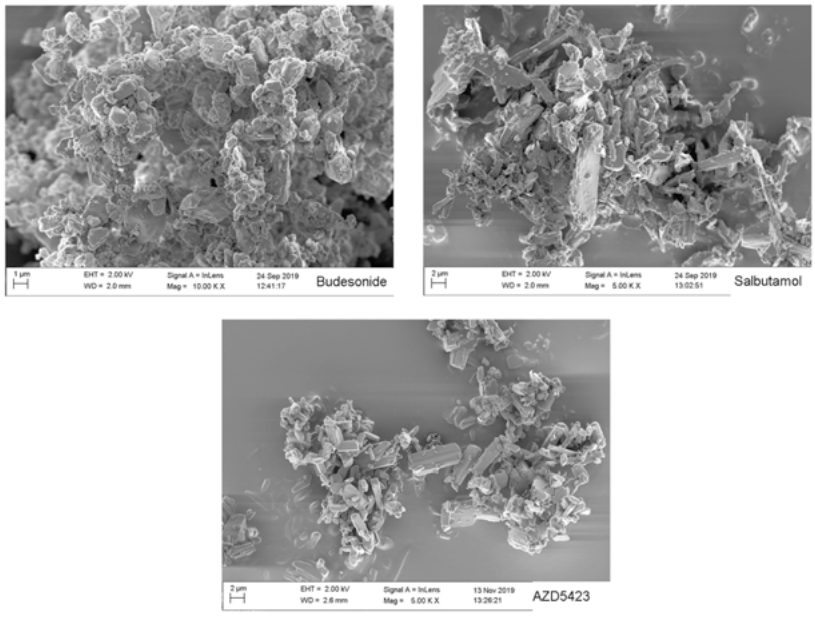

Figure 11. SEM images of the active pharmaceutical ingredients taken at 5000–10,000x magnification.

Relationships between surface coverage ratio and powder mechanics

In this thesis, mixtures with surface coverage ratios (SCR) between 0 and 6 were used. In the first two papers (both concerning the powder mechanics of carriers with increased SCR of lactose fines), the relationships between the surface coverage ratio and this measure's impact on the powder mechanics were extensively investigated. In the first paper, the mechanics of these adhesive mixtures were studied using an array of different techniques. It was found that the dynamics and the spatial distribution of the fines on the carrier particles changed with increased SCR. Figure 12 (adapted from **Paper I**) illustrates how the adhesive units arrange under unsettled conditions (a) and under compression (b). It was found that, with small additions of fines (SCR 0.25), there was an increase in unsettled bulk density, or *carrier density* (a), due to adhesion of fines onto (and into) the irregularities and open pores of the Lactopress carrier. This adhesion effectively lead to a densification of the adhesive units and a smoothening of the particles leading to improved packing (85, 103). The term *active sites* has been used to describe these locations on the carrier, because the fines also tend to adhere strongly to these sites (44, 84, 104). With further additions of fines, an adhesion layer started to form on the outer, enveloped, surface of the carrier. This adhesion layer grew in complexity with higher SCRs, thus leading to increased spacing between the adhesive units, resulting in a lower bulk density. When exposed to compression, either from increased normal stresses or from tapping, the adhesive units were prone to rearrangement (b). With increased complexity of the adhesion layer, the more the adhesive units were sensitive to compression forces, as indicated by a relatively higher increase in bulk or carrier density.

From all the different techniques used to assess the powder mechanics (**Paper I)**, it was concluded that similar results, in terms of rank order between the mixtures, could be obtained using several techniques. However, there were some differences among the techniques that could be linked to the type of flow mechanism used during the measurement (i.e. compression flow or convective flow). It has been suggested that the type of powder mechanical testing technique used should preferably match the targeted handling or manufacturing procedure (105).

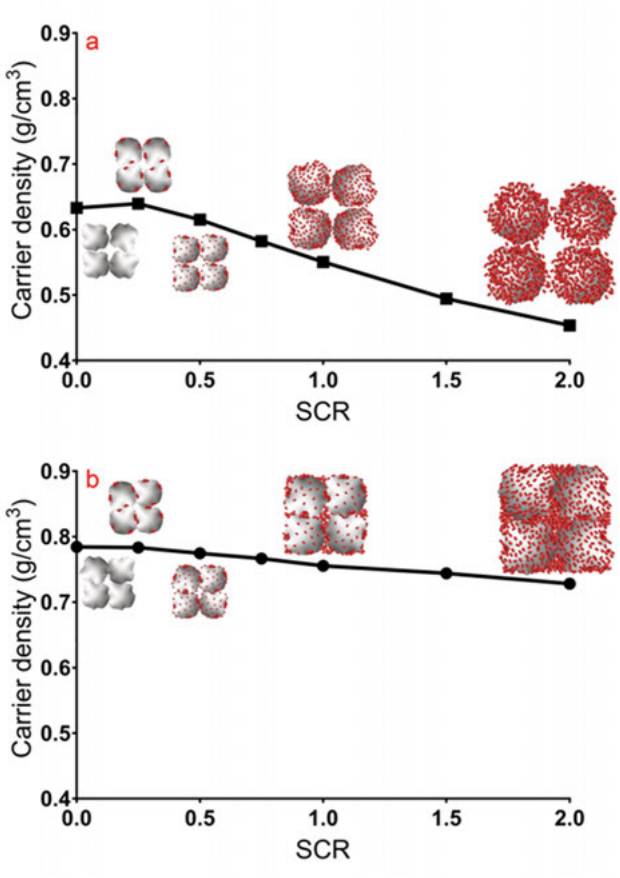

Figure 12. The spatial distribution of carrier and fine particles (forming an adhesive unit) at unsettled (a) and compressed (b) conditions. The carrier density is calculated as: $Carrier\ density = UBD\ (1-f)$ where f is the fraction of fines.

The blend state model

Based on **Paper I**, the *blend state model* (Figure 13) was proposed. This model is based on the evolution of the blend state with increased drug loads or increased SCRs. The different states express the dynamics and appearance of the adhesive units as described in the previous section. The model posits four different states. In the first state, denoted *S1*, the fines adhere to the irregularities, inner surfaces or open pores of the carrier particles. This process makes the adhesive units denser, because the volume of the units remains the same while the mass increases. In the second state, denoted *S2*, the fines particles start to adhere to the enveloped surface, forming an adhesion layer, which increases the volume of the adhesive unit. S2 can be further sub-divided into two sub-states depending on the dynamics of the adhesion layer. In *S2a*, the adhesion layer is relatively stable and insensitive to restructuring during com-

pression and shearing of the blend. In *S2b*, the growing adhesion layer is responsive to external stresses and the fines are prone to rearrange and to migrate. In the final state, denoted *S3*, a free fraction of self-agglomerates appear that are no longer attached to the carrier. These self-agglomerates are spontaneously formed during mixing in a system that is oversaturated by fines (58, 106, 107) and is by definition a segregated state.

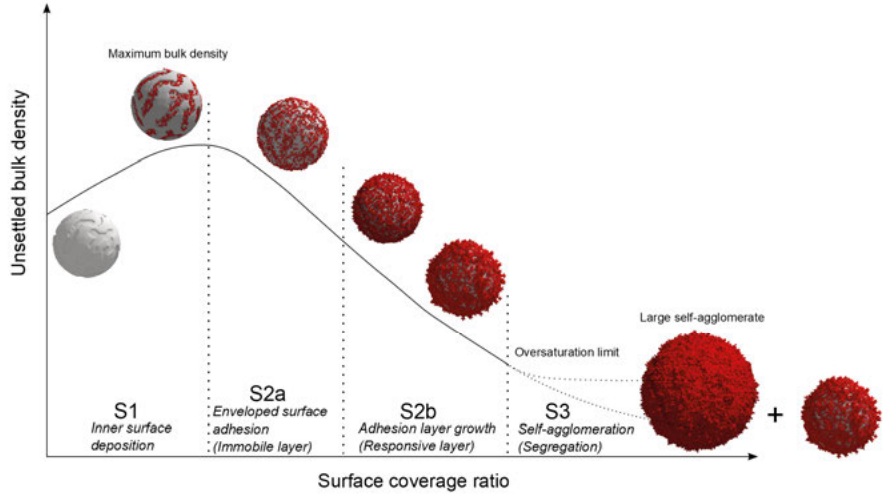

Figure 13. The blend state model consisting of four different states of an adhesive mixtures dependent on the surface coverage ratio.

To identify the states of the blend state model, a combination of both powder mechanical analysis and imaging techniques was required. The maximum unsettled bulk density or improved packing defines the first state. Both sub-states of the second state are defined partly by a decrease in unsettled bulk density or flowability and partly by the appearance of the adhesive units. The final state can easily be recognized visually, because at this state, large self-agglomerates are present. Using the blend state model, the different states of the carrier particles expressed in **Paper II** could be identified and presented as *blend state maps* (see next section). In addition, blend state maps of the different APIs used in **Paper III** could be formed.

Blend state maps

In order to get an overview of the evolution of the blend state between different adhesive mixtures, a blend state map can be used. In **Paper II**, a blend state map of the adhesive mixtures based on the five different carriers was created (Figure 14), while in **Paper III,** a blend state map of the different API mixtures was made (Figure 15). The horizontal lines on the maps indicate the range of SCRs in-between which a certain blend state was observed. A transition interval between two observed states is described by a dashed line with a slope and within this interval, the transition to the next state occurs. The *exact* point (SCR or fines content) of a transition is unknown, because a limited number of blends were studied, and the SCR range of the transition interval thus depends on the frequency of the data points and will vary depending on the experimental design. In the map depicting the carriers as presented in **Paper II** (Figure 14), it can be seen that the maximum drug load (SCR) and extension (length) of each state varies among carries (recall from Table 1 that the carriers can be grouped in two categories, namely large and small). However, the difference in the blend state maps can not be fully explained by the size differences alone. Other factors such as the surface roughness and other morphological aspects played an important role; for example, the Lactopress carrier behaved quite differently than the other smaller carriers. Similarly, the larger carriers Inhalac 70 and Respitose SV001 behaved differently from each other.

The combination of morphological irregularities (like surface pores to express the S1 state, together will surface roughness) appeared to be beneficial for higher drug loads. In a study by Hertel et al. (84), similar observations were made where larger, more irregular carriers could handle higher drug loads than smaller and smoother carriers. In the case of Respitose SV001, which had a similar shape to Respitose SV010 and Inhalac 230, the larger size appears to be beneficial in terms of de-agglomeration during mixing (52, 108). Hence, higher drug loads before the mixture segregated due to self-agglomeration (i.e., state S3) could be reached.

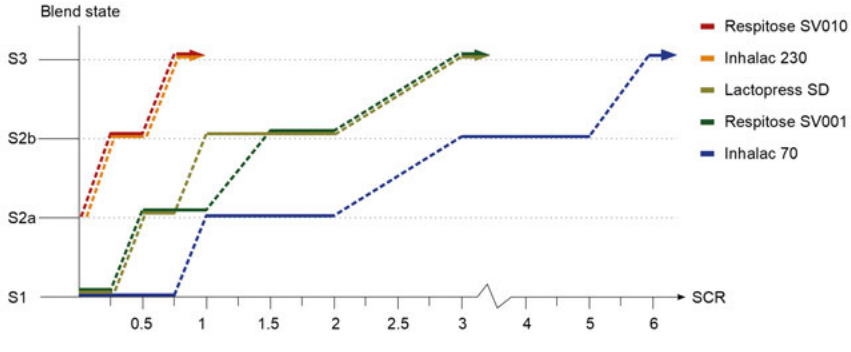

Figure 14. Blend state maps over the expressed blend states of each carrier mixture in relation to the SCR (presented in **Paper II**).

In **Paper III**, different blend state maps for each fines material were obtained when varying the drug content, similar to the carrier map in **Paper II** (Figure 15). This pattern indicates that it is not only the carrier that determines the evolution of the blend state, but also the type of drug used. The shape of the fines particles, as well as the structure of the adhesion layer that was formed, could explain the differences in the blend state maps between the fines. Budesonide yielded a relatively uniform and coherent adhesion layer on the carrier surface, while salbutamol gave a thick uneven layer of low density characterised by small agglomerates dispersed on the carrier surface. The particles of salbutamol were needle shaped (Figure 11), which have been found to be harder to pack into pores than more spherical particles (48, 109). This morphology of the particles resulted in a lower content of fines in the S1 state compared to budesonide, which appeared to have a higher packing density into the pores (i.e., there were more fines). The total loading capacity was also highest for budesonide, as indicated by the fact that the concentration before reaching S3 was the highest of the APIs. AZD5423 developed an adhesion layer thickness similar to budesonide, but the layer was more heterogeneous in structure with patches of agglomerated fines attached to the carrier instead of a more continuous layer of fines. Moreover, AZD5423 was more prone to self-agglomerate, and achieved the S3 state at a much lower fines concentration than budesonide.

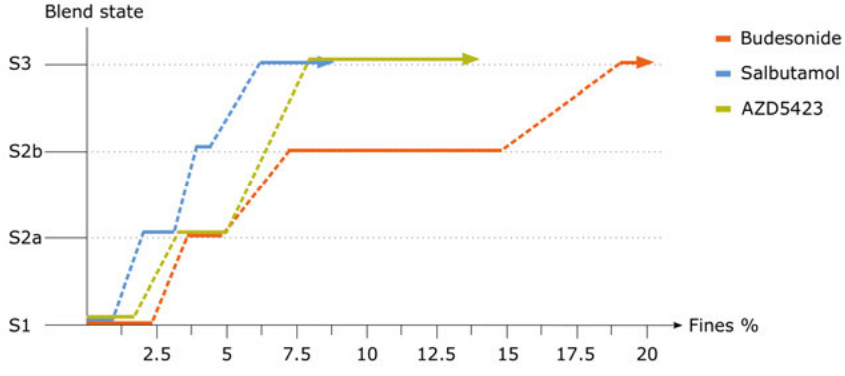

Figure 15. Blend state maps over the expressed blend states of each fines mixture in relation to fines content (presented in **Paper III**).

In conclusion, a blend state map provides information about critical transition points and fines concentration ranges that affect the formulation performance. Firstly, the proportions of fines located in pores (which may subsequently be difficult to disperse) is indicated by the S1 state. Secondly, the concentration range of fines within which the powder flowability can be expected to change is given by the duration of the S2 state. Thirdly, the probability that adhered fines may migrate during powder densification (in e.g. a filling process) will increase significantly when a state transition occurs from S2a to S2b. Finally,

as estimate is given for the point at which the segregated and unacceptable blend state S3 (which represents and upper limit of drug load) will be reached.

Blend state / dispersibility relationships

In **Papers III** and **IV**, the focus shifted from blend state/powder mechanics to blend state/dispersibility relationships. In **Paper III**, the dispersibility, or aerosolization performance, was studied for adhesive mixtures containing three APIs using one flow rate. After forming the blend state map presented in the previous section (Figure 15), the dispersibility of the three API mixtures was linked to the evolution of the blend state.

In Figure 16, the dispersibility is presented as the fine particle fraction (FPF). As can be seen, the dispersibility profiles of the APIs could be divided into three regions, each coupled to the blend state of the adhesive mixtures. In S1, the fines particles are located in open cavities and a low FPF is obtained. The particles are shielded and also relatively strongly adsorbed on the surface inside the cavities and will detach to a limited degree during dose withdrawal. When the surface cavities are gradually filled, the particles become less shielded and the FPF increase markedly with fines concentration. That the FPF for particles located in surface cavities is relatively low and will increase when an adhesion layer at the outer carrier surface is formed has been reported previously (61, 81, 84). In S2, the FPF continues to increase, but at a gradually decreasing rate, and approaches a constant FPF with increased fines concentration, the latter coinciding with the transition out of S2b into S3. Finally, S3 is characterized by a nearly constant or even falling FPF. In this state, large self-agglomerates exist that will resist disintegration and dispersion in the air, especially when using an inhaler of a ScreenHaler type, which lacks impaction surfaces (99). Self-agglomerates will thus be emitted from the inhaler and subsequently impact in the throat or the pre-separator (81, 84, 110). The formation of a gradually thicker and more uneven adhesion layer in S2 thus facilitates detachment of fines. However, at the beginning of S3, an adhesion layer of unaltered structure has been formed, and further addition of fines will increase the concentration of free self-agglomerates that are difficult to disintegrate, and FPF will remain constant.

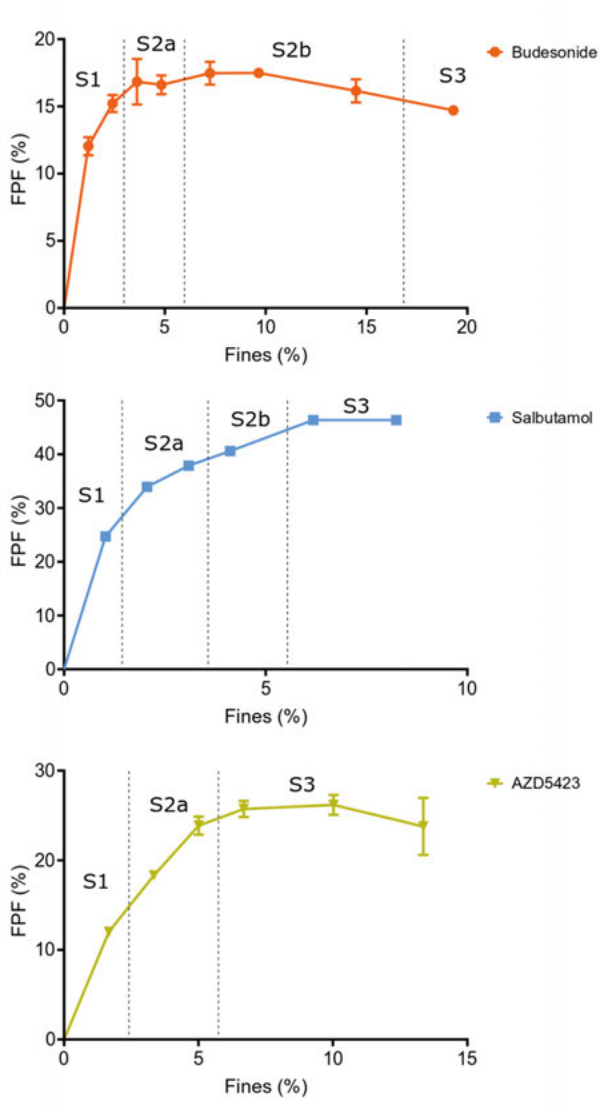

Figure 16. Dispersibility presented as the fine particle fraction (FPF) for budesonide-, salbutamol-, and AZD5423-containing mixtures in relation to the proportion of fines. Note that the y- and x-axes are different for each API.

The different detachment mechanisms from each state during inhalation are summarized in Figure 17 (similar mechanisms have also been noted, e.g. (81, 84, 111)). In the S1 state, the fines particles are released from the cavity as single particles, albeit to a low extent because they are shielded from the airflow (61, 68). In the S2a state, the fines are also predominantly released as single particles, but because they are more exposed to the air, they detach more easily (81). In the agglomerated states S2b and S3, a combination of single

particles and agglomerates of fines will detach from the carrier surfaces (70, 99).

It is concluded that the structure of the adhesion layer is an important factor explaining the relationship between blend state and blend dispersibility. It is reasonable that the nature of the API is critical for the development of the adhesion layer structure. For the APIs used in this study, the particle sizes were similar, but there were differences in particle shape, and this property of an API might explain the observed differences in blend dispersibility. That is, an elongated particle shape tend to form a more porous and heterogeneous adhesion layer, which facilitates the detachment and dispersion processes during aerosolization (48, 64). However, other API properties may also be important, such as the surface energy affecting the strength of the adhesive and cohesive interactions in the blend (112, 113).

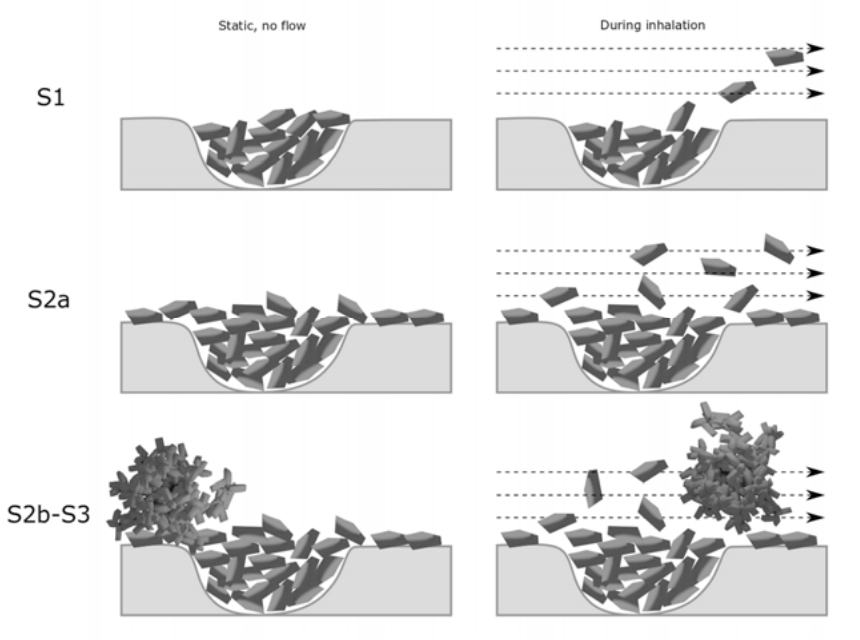

Figure 17. The putative detachment mechanisms at each state during inhalation. In the S1 state, the fines are sheltered from the airflow. In the S2a state, the particles are more exposed and detach as single particles. In the more complex adhesion layer in S2b and S3, the fines detach as clusters or smaller agglomerates.

Effect of pressure drop on the dispersibility

In the fourth and final project, the effect of pressure drop on the blend state/ dispersibility relationship was investigated. The pressure drop was set to 0.5, 2 or 4 kPa during the impaction experiment, and the budesonide containing mixtures were expelled through a ScreenHaler device with a *Turbuhaler*® mouth piece. The findings are summarized in Figure 18, which shows the dispersibility from each blend state at the tested pressure drops. The figure demonstrates that, once a *critical pressure drop* had been reached, the blend state dispersibility seemed to be independent of the flow rate (2 kPa), but instead more dependent on the adhesion layer structure in state S2a and subsequent states (as discussed in the previous section). However, it is known that different types of inhaler geometries can affect the dispersion capacity (47, 82). Thus, a different critical pressure drop would probably be found with another inhaler device.

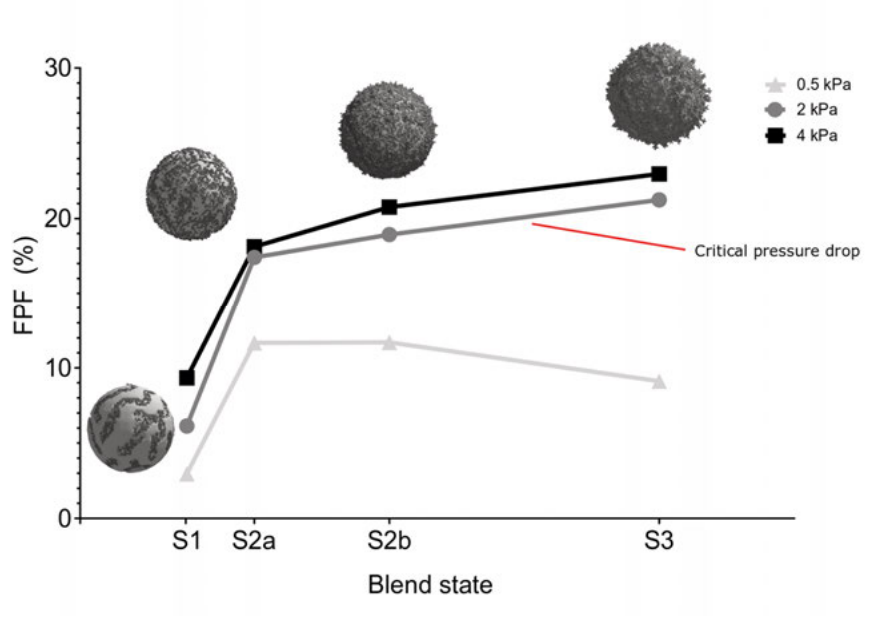

Figure 18. Dispersibility of the different states as a function of the pressure drop.

In addition to the effect of the pressure drop, a ternary mixture ($S2a_{only}$) containing lactose fines up to S1 (SCR 0.25) and then budesonide fines corresponding to a SCR of 0.5 was made. Adding inert fines to fill the open pores to improve the dispersibility is a well-known technique employed when formulating adhesive mixtures for inhalation (70, 114, 115). Thus, using the S1 blend state to determine the amount of fines to use could prove to be a useful formulation strategy. It was found that this ternary mixture indeed increased the FPF compared to the S1 binary mixture of budesonide, and gave rise to a

bended dispersibility profile similar to the S2a mixtures and above (Figure 19). It is clear that the dispersibility of the S1 mixture is directly proportional to the pressure drop, while at state S2 or higher, the adhesion layer structure was more important. It is known that when a thicker adhesion layer is formed, fines-to-fines cohesion rather than fines-to-carrier adhesion will control the release of fines (70). However, the fines in the adhesion layer are more exposed to press-on forces, which can result in a reduction in FPF (58, 70). As for the ternary $S2a_{only}$ composition, this mixture was mixed for twice as long, which could explain why it had a lower FPF than S2a mixture (69, 75).

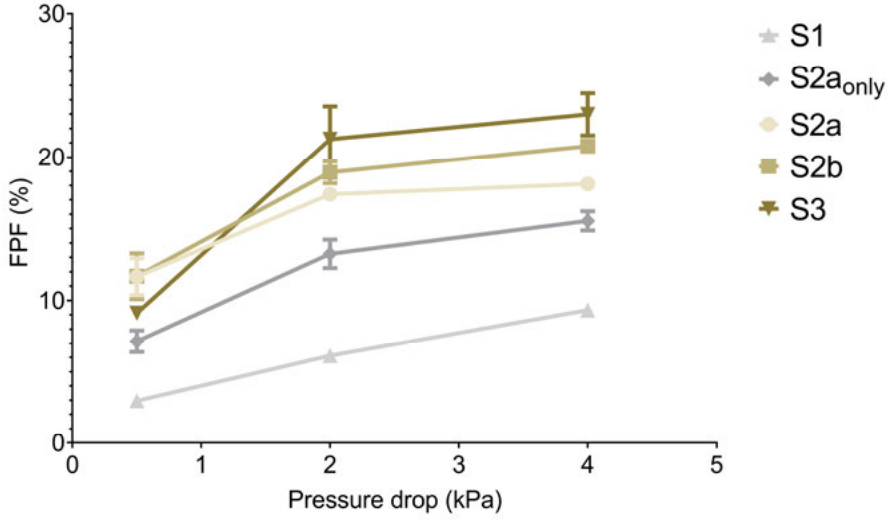

Figure 19. The fine particle fraction (FPF) of each mixture at different pressure drops.

Implications for formulation and applicability of the blend state model

In **Papers I** and **II** outlining the blend state model, the focus was on the powder mechanics of the adhesive mixtures corresponding to the different states. It was found that the mobility of the fines located in the adhesion layer increased with a thickening adhesion layer and at a critical point, segregation in the form of large self-agglomerates would occur. Mapping the evolution of the blend state into a blend state map provides information about critical factors of adhesive mixtures that are to be used as inhalation powders. Examples of such factors are the amount of fines that can be located in pores of carrier particles, the concentration range of fines within which the powder flowability can be expected to change, the maximum fines load before segregation occurs, and the probability of fines migration during powder densification (in e.g. a filling process). The blend state map is thus a potentially important tool for characterising adhesive mixtures and predicting formulation performance, e.g. for the filling of inhaler devices and inhalation performance regarding dosing, dose detachment, and de-agglomeration of fines

The segregated S3 state could behave a bit differently depending on the size and number of the self-agglomerates. Formulation-wise, the S3 state is a segregated and undesirable state even though no major issues were noticed regarding the dispersibility or homogeneity of the studied blends. However, in a reservoir device, a larger dose variation due to significant segregation of the S3 state could be obtained than was seen in our single-dose inhaler. With the $S2a_{only}$ mixture, the idea was to show the applicability of identifying the width of the S1 state. When adding inert fines corresponding to the S1 state, the open pores of the carriers would be filled and the added drug would end up in the enveloped layer of the S2 state, thus leading to improved dispersibility. In the commercial formulation of adhesive mixtures, it is common formulation practice to add inert fines to improve the dispersibility. However, exactly how much fines is needed depends on the carrier-API combination used, and usually requires some trial and error during formulation. The use of a blend state map could thus potentially be a tool for identifying how much fines is needed to fill the pores and to identify the usable range of fines (i.e. up to the point of self-agglomeration, S3). However, the mechanisms behind the use of inert fines appears more complex than just filling the pores, as the added fines also appear to form co-agglomerates with the APIs, which can affect the dispersibility (62, 87, 114).

Conclusions

In this thesis, critical properties of adhesive mixtures have been identified and summarized in a blend state model that describes the spatial distribution of fines and carrier particles in an adhesive mixture. The model consists of four distinct states with inherent properties and identifiers. In the first state, S1, the fines deposit on the inner surfaces of the carrier, giving an increase in mass of the adhesive units but an unchanged enveloped volume, which is reflected as an increased bulk density of the blend. In the second state, S2a, the fines will predominantly adhere to the outer carrier surface, which increases the enveloped volume of the ordered units and consequently increases the separation distance between the carriers. This state is characterized by a relatively stable adhesion layer. Following further additions of fines (i.e. increased surface coverage ratio), the adhesion layer grows in thickness and complexity and the next state, S2b, is reached. This state is defined by a more responsive adhesion layer that is more sensitive to compression and rearrangement during handling. In the final state, S3, the adhesive units are oversaturated with fines, which results in the formation of large fines agglomerates (i.e. self-agglomerates). This state is by definition a segregated state, which may lead to abrupt changes in the powder mechanics depending on the specific carriers and fines used. It was found that the number of expressed states and the surface coverage ratio at which the transitions between different states occurred varied depending on the properties of the carriers and the fines. The findings were summarized in blend state maps, expressing the evolution of the blend state as a function of surface coverage ratio (SCR) or drug content. This map is proposed for representing and describing all individual carrier-fines systems.

Based on this work, it was also concluded that the diameter and volume of the pores on the carrier surfaces dictated the existence and duration of the S1 state in addition to the size and morphology of the fine particles. The S2 and S3 states, and the duration of S2, varied depending on the sizes and morphologies of the carriers and fines used. Carriers with a larger size and rougher surfaces were found to be more proficient in de-agglomerating fines during mixing, thus extending the SCR until the S3 state was reached. More uneven particle shapes of the fines gave rise to a less dense and coherent adhesion layers in states S2a and b.

In the second part of the thesis studying the blend state/dispersibility relationships, it was found that the dispersion degree in the different blend states, i.e. the absolute levels of fines particle fraction or fines particle dose, differed

among the drugs, and this difference was especially notable in state S2. Thus, the structure of the adhesion layer was important for dispersibility. For the S1 blend state, where the fines are located in the cavities and open pores of the carrier, the fines particles were strongly bonded to the carrier and difficult to detach. In this state, the degree of dispersion was found to be linearly related to the pressure drop. However, when an outer adhesion layer had started to form, i.e. in blend states S2a and higher, the pressure drop was less important to the dispersion once a critical pressure drop had been reached. Above this level of pressure drop, variations in the degree of dispersion were more affected by the blend state than by the airflow rate.

The findings presented in my thesis can be summarized in an illustration that shows the interplay of the different factors that ultimately influence dispersibility (Figure 19). My hope is that the blend state model and the blend state maps will ultimately become important tools for aiding the characterisation of adhesive mixtures, which will help us predict formulation performance in such processes as device filling and dispersibility (i.e. dose detachment and de-agglomeration of fines), thus improving formulation work.

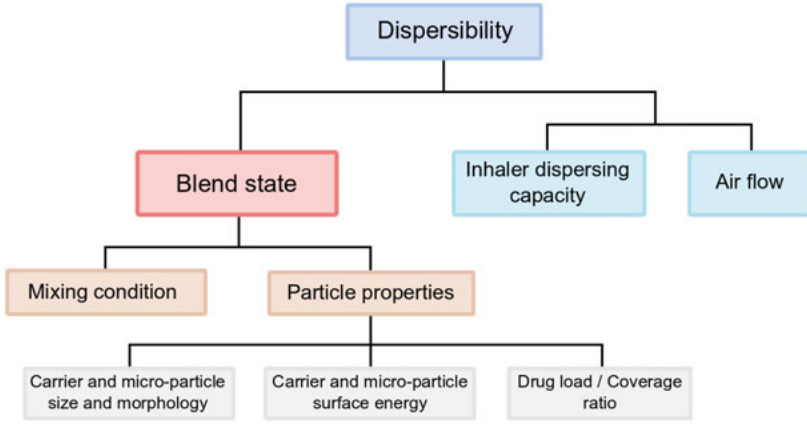

Figure 20. Schematic of the factors influencing the dispersibility of a dry powder inhaler formulation from the perspective of this thesis.

Future perspectives

The field of pulmonary drug delivery is continually growing, with an overall aim of filling un-met medical needs, both for treat severe respiratory diseases and for novel treatments of systemic conditions such as diabetes. The pulmonary route has great potential both for local targeting of lung diseases, but also for the delivery of protein and peptide drugs that would undergo extensive and damaging metabolism through the oral route. A general aim when formulating inhaled drugs is to achieve as high delivered drug dose as possible. Traditionally, adhesive mixtures have been used for potent drugs delivered in low doses. However, for non-potent drugs, the drug load must be increased to avoid the need of several actuations to reach the therapeutic dose. Using the blend state model, tuning the formulation for the optimal drug concentration could potentially be accomplished. The use of a blend state map would allow an overview of the particular adhesive mixture and provide for easier comparison between systems.

However, some knowledge gaps still exist about the blend state model, and further work is needed to fully develop the usefulness of the blend state model from both a manufacturability (i.e. related to the first two papers) and dispersibility aspect. Such studies could focus on the relationships between the blend state and mixing, as well as the influence of various press-on forces under mixing on the dispersibility and evolution of the blend state. In addition, the geometries of different inhaler devices could be investigated, to help us learn about the detachment mechanisms at each state under varied conditions. Tin this thesis, the blend state/dispersibility relationships were studied using only one type of carrier, and as was seen in the first part of the thesis, the carrier properties will give rise to different blend state maps. Hence, to further study the dispersibility relationship, more varied sets of carriers would be needed to be studied.

With the limitations of some patients to produce sufficient pressure drops during inhalation, the findings of a critical pressure drop for specific formulations could prove useful to formulate DPI powders that are less airflow dependent. This aspect would be further needed to be expanded upon using other types of drugs, carriers and inhaler devices.

Populärvetenskaplig sammanfattning

Tillförseln av läkemedel via inandning kan spåras långt tillbaka i tiden. I forntiden rörde det sig främst om att inhalering av diverse växtbaserade läkemedel via rökning men i modern tiden, från ca 1950-talet, har flera revolutionerande framsteg inom läkemedelstillförsel via luftvägarna gjorts. Numera inhalerar främst patienter med visad farmakologisk effekt för att behandla sjukdomar som astma och kronisk obstruktiv lungsjukdom (KOL). Det finns flera olika typer av inhalatorer på marknaden idag så som nebulisatorer, inhalationssprayer och pulverinhalatorer där den sistnämnda på senare år har blivit mer populär på grund av hög användarvänlighet och längre hållbarhetstid. Det finns olika sätt att formulera inhalationspulver på men ett av de vanligaste sätten är att skapa s.k. ordnade blandningar. I dessa används stora inerta partiklar (bärare) och små mikrometerstora läkemedelspartiklar. När de två partikeltyper blandas så fäster de små läkemedelspartiklarna spontant på ytan av de stora bärarpartiklarna. Vid själva inhalationsförfarandet lossnar läkemedelspartiklarna från bärarna och följer med luftströmmen ner i lungorna där de kan utöva sin tilltänkta effekt. Bärarna, som ofta består av laktos, är för stora för att nå lungorna och hamnar istället i svalget för att sedan sväljas.

Vid formulering av dessa ordnade blandningar är det viktigt att attraktionskraften mellan bärare och läkemedel är tillräckligt hög för att inte börja separera under tillverkning eller transport, men samtidigt tillräckligt låg för att kunna separera under inhalationsförfarandet. Beroende på läkemedelsmängden i blandningen förändras balansen mellan läkemedel- och bärarpartiklarna och olika blandningsstrukturer eller tillstånd uppstår. Vid låga andelar uppnås ett blandningstillstånd där läkemedlet främst letar sig in i porer eller ojämnheter på ytan av bärarna. Vid högre andelar läkemedel byggs succesivt ett lager av läkemedelspartiklar upp på bärarytan med ökad komplexitet beroende på läkemedelsmängden. Vid mycket höga mängder så tenderar läkemedlet att segregera och bilda egna klumpar istället för att fortsätta fästa på bärarna. Detta steg är oönskat, då det kan leda till höga dosvariationer.

I studien undersöktes de olika blandningstillstånden utifrån mekanisk stabilitet hos blandningen vid olika ration av läkemedel:bärare samt vid användandet av olika typer av bärare och läkemedelspartiklar. Slutsatserna av detta var att större och mer ojämna bärarpartiklar kunde hantera högre koncentrationer av läkemedelspartiklar innan segregering av blandningen började uppstå. Dessa egenskaper hos bärarna hjälpte till att riva sönder klumpar av läke-

medel under blandningen och således motverkade bildandet av större läkemedelsklumpar. Vid användandet av olika typer av läkemedelspartiklar drogs slutsatsen att ojämnt formade partiklar ledde till uppbyggnaden av ett mer poröst lager på bärarytan. Detta begränsade mängden läkemedelspartiklar som kunde användas i blandningen innan segregation började uppstå. De olika blandningstillstånden som uppstod för varje bärare och varje läkemedelspartikel kunde slutligen kartläggas i en blandningstillståndskarta där det enkelt gick att följa blandningstillståndets utveckling i förhållande till proportionen av läkemedel.

I studien undersöktes även läkemedelspartiklarnas benägenhet att lossna från bärarna under ett inhalationsförfarande (dispergerbarheten). Dispergerbarheten undersöktes också vid olika luftflöden för att bättre förstå skillnader hos de olika blandningstillstånden. Detta är också intressant ur ett patient perspektiv då inandningsförmågan kan variera från patient till patient. Slutsatsen av detta var att de läkemedelspartiklar som bildade ett poröst lager på bärarna lättare lossnade under inhalation samt att partiklar som satt i porerna på bärarna hade svårt att lossna. Det noterades även att ett visst kritiskt luftflöde behövde uppnås för att ordentligt kunna dispergera en ordnad blandning.

Användandet av de olika blandningstillstånden som en förklaringsmodell samt kartläggandet av utvecklingen av blandningstillstånden visade sig vara användbara verktyg för att karakterisera ordnade blandningar och förstå kritiska egenskaper som är viktiga både vid tillverkning och vid inhalation. Målet med denna förklaringsmodell är att underlätta formuleringsarbetet av inhalationsläkemedel för att i slutändan kunna uppnå säkrare och effektivare behandlingar för patienter.

Acknowledgements

The work conducted in this thesis was performed at the department of Pharmaceutical Biosciences, Faculty of Pharmacy, Uppsala University, as a part of the Swedish Drug Delivery Forum (SDDF).

I would like to extend my gratitude to AstraZeneca Gothenburg, which sponsored this project. In addition, I would like to express my appreciation to IF stiftelsen inkl Källrotstipendiet (Apotekarsocieteten) and Apotekare C D Karlssons stiftelse (Apotekarsocieten) for giving me travelling grants.

First and foremost, I would like to thank my main supervisor Göran Alderborn (UU) for great guidance and scientific input, my co-supervisor Göran Frenning (UU) for assistance, and my industrial co-supervisors Kyrre Thalberg (AZ, Emmace) and Tobias Bramer (AZ) for expert opinions and for providing support regarding materials and equipment.

In my day-to-day work in the lab, my gratitude is extended towards Lucia Lazorova (UU) who has been a helping hand with everything from acquiring materials to taking SEM pictures.

For the work involving pharmaceutical impactors, I would sincerely like to thank Patrik Andersson (AZ) for excellent support and expert knowledge and Jan-Olof Svensson (AZ) for detailed support regarding the chemical analysis and quantification. In this context, I would also like to thank Johan Gråsjö (UU) for support with post-processing of data and calculations.

I would also like to thank the PhD students in the Pharmaceutics group *Irès*, *Sohan*, *Sara*, *Maryam*, *Marilena* and *Anna* for providing a great working environment. Special thank you to *Irès* and *Sohan* for all the fun times we have had at work, at conferences and off work!

Much gratitude is also extended to my former PhD student colleagues at the department of Pharmacy for everything fun and interesting that has happened both on and off work! Muchas gracias to *Vicky*!

To my now good friends *Caroline* and *Johanna*: thank you for taking care of me as a lost gothenborgian when I first came to Uppsala. I would also like to thank you for all the great times and support! It has been a blast getting to know you!

To my family. Tack så mycket mamma och pappa för all hjälp och uppmuntran! Även ett stort tack till min syster Linda som hälsat på mig ibland! Utan er hade det inte gått!

References

1. Dessanges J-F. A history of nebulization. Journal of aerosol medicine. 2001;14(1):65-71.
2. Hinds WC. Aerosol technology: properties, behavior, and measurement of airborne particles: John Wiley & Sons; 1999.
3. Hickey AJ, Conway J. Historical perspective–Disruptive technologies and strategies. Inhaled Medicines. 2021:1-12.
4. Pitance L, Vecellio L, Leal T, Reychler G, Reychler H, Liistro G. Delivery efficacy of a vibrating mesh nebulizer and a jet nebulizer under different configurations. Journal of aerosol medicine and pulmonary drug delivery. 2010;23(6):389-96.
5. de Boer AH, Thalberg K. Devices and formulations: General introduction and wet aerosol delivery systems. Inhaled Medicines: Elsevier; 2021. p. 35-63.
6. Newman SP. Principles of metered-dose inhaler design. Respiratory care. 2005;50(9):1177-90.
7. de Boer A, Hagedoorn P, Hoppentocht M, Buttini F, Grasmeijer F, Frijlink H. Dry powder inhalation: past, present and future. Expert opinion on drug delivery. 2017;14(4):499-512.
8. de Boer AH, Thalberg K. Dry powder inhalers (DPIs). Inhaled Medicines: Elsevier; 2021. p. 99-146.
9. Labiris N, Dolovich M. Pulmonary drug delivery. Part I: physiological factors affecting therapeutic effectiveness of aerosolized medications. British journal of clinical pharmacology. 2003;56(6):588-99.
10. Wang Y-B, Watts AB, Peters JI, Williams III RO. The impact of pulmonary diseases on the fate of inhaled medicines—A review. International journal of pharmaceutics. 2014;461(1-2):112-28.
11. Aulton ME, Taylor KM. Aulton's Pharmaceutics E-Book: The Design and Manufacture of Medicines: Elsevier Health Sciences; 2017.
12. Hickey AJ, da Rocha SR. Pharmaceutical inhalation aerosol technology: CRC Press; 2019.
13. Roberts DL, Mitchell JP. Measurement of aerodynamic particle size distribution of orally inhaled products by cascade impactor: how to let the product specification drive the quality requirements of the cascade impactor. AAPS PharmSciTech. 2019;20(2):1-10.
14. Forbes B, Bäckman P, Christopher D, Dolovich M, Li BV, Morgan B. In vitro testing for orally inhaled products: developments in science-based regulatory approaches. The AAPS journal. 2015;17(4):837-52.
15. Zeng XM, Martin GP, Marriott C. Particulate Interactions in Dry Powder Formulation for Inhalation: CRC Press; 2000.
16. Newman SP. Aerosol deposition considerations in inhalation therapy. Chest. 1985;88(2):152S-60S.
17. Marieb EN, Hoehn K. Human anatomy & physiology. 8th ed: Pearson education; 2010.

18. Tu J, Inthavong K, Ahmadi G. The human respiratory system. Computational fluid and particle dynamics in the human respiratory system: Springer; 2013. p. 19-44.
19. Patton JS. Mechanisms of macromolecule absorption by the lungs. Advanced drug delivery reviews. 1996;19(1):3-36.
20. Enlo-Scott Z, Swedrowska M, Forbes B. Epithelial permeability and drug absorption in the lungs. Inhaled Medicines: Elsevier; 2021. p. 267-99.
21. WHO. Chronic obstructive pulmonary disease (COPD) https://www.who.int: World Health Organization; 2017 [Available from: https://www.who.int/news-room/fact-sheets/detail/chronic-obstructive-pulmonary-disease-(copd).
22. WHO. Asthma www.who.int: World Health Organization; 2020 [Available from: https://www.who.int/news-room/q-a-detail/asthma.
23. WHO. Burden of COPD www.who.int: World Health Organization; 2020 [cited 2020 2020-08-31]. Available from: https://www.who.int/respiratory/copd/burden/en/.
24. Pearce N, Aït-Khaled N, Beasley R, Mallol J, Keil U, Mitchell E, et al. Worldwide trends in the prevalence of asthma symptoms: phase III of the International Study of Asthma and Allergies in Childhood (ISAAC). Thorax. 2007;62(9):758-66.
25. Horne R. Compliance, adherence, and concordance: implications for asthma treatment. Chest. 2006;130(1):65S-72S.
26. Rodrigo GJ, Rodrigo C. The role of anticholinergics in acute asthma treatment: an evidence-based evaluation. Chest. 2002;121(6):1977-87.
27. Barnes PJ. Mechanisms in COPD: differences from asthma. Chest. 2000;117(2):10S-4S.
28. Renkema TE, Schouten JP, Koëter GH, Postma DS. Effects of long-term treatment with corticosteroids in COPD. Chest. 1996;109(5):1156-62.
29. Mahler DA, Donohue JF, Barbee RA, Goldman MD, Gross NJ, Wisniewski ME, et al. Efficacy of salmeterol xinafoate in the treatment of COPD. Chest. 1999;115(4):957-65.
30. Calverley PM, Stockley RA, Seemungal TA, Hagan G, Willits LR, Riley JH, et al. Reported pneumonia in patients with COPD: findings from the INSPIRE study. Chest. 2011;139(3):505-12.
31. Ferkol T, Schraufnagel D. The global burden of respiratory disease. Annals of the American Thoracic Society. 2014;11(3):404-6.
32. Scherließ R. Future of nanomedicines for treating respiratory diseases. Expert opinion on drug delivery. 2019;16(1):59-68.
33. Knowles MR, Durie PR. What is cystic fibrosis? : Mass Medical Soc; 2002.
34. Crompton G. A brief history of inhaled asthma therapy over the last fifty years. Primary care respiratory journal. 2006;15(6):326-31.
35. Stein SW, Thiel CG. The history of therapeutic aerosols: a chronological review. Journal of aerosol medicine and pulmonary drug delivery. 2017;30(1):20-41.
36. Sanders M. Inhalation therapy: an historical review. Primary care respiratory journal. 2007;16(2):71-81.
37. Stanbury RM, Graham EM. Systemic corticosteroid therapy—side effects and their management. British Journal of Ophthalmology. 1998;82(6):704-8.
38. Newman S, Busse W. Evolution of dry powder inhaler design, formulation, and performance. Respiratory medicine. 2002;96(5):293-304.
39. Usmani OS, Scullion J, Keeley D. Our planet or our patients—is the sky the limit for inhaler choice? The Lancet Respiratory Medicine. 2019;7(1):11-3.

40. Geller DE. Comparing clinical features of the nebulizer, metered-dose inhaler, and dry powder inhaler. Respiratory care. 2005;50(10):1313-22.
41. Mukhopadhyay A, Waked M, Gogtay J, Gaur V. Comparing the efficacy and safety of formoterol/budesonide pMDI versus its mono-components and other LABA/ICS in patients with asthma. Respiratory Medicine. 2020:106055.
42. Healy AM, Amaro MI, Paluch KJ, Tajber L. Dry powders for oral inhalation free of lactose carrier particles. Advanced drug delivery reviews. 2014;75:32-52.
43. de Boer AH, Chan H, Price R. A critical view on lactose-based drug formulation and device studies for dry powder inhalation: which are relevant and what interactions to expect? Advanced drug delivery reviews. 2012;64(3):257-74.
44. Grasmeijer F, Grasmeijer N, Hagedoorn P, Willem Frijlink H, Haaije de Boer A. Recent advances in the fundamental understanding of adhesive mixtures for inhalation. Current pharmaceutical design. 2015;21(40):5900-14.
45. Pilcer G, Amighi K. Formulation strategy and use of excipients in pulmonary drug delivery. International journal of pharmaceutics. 2010;392(1):1-19.
46. Zhou QT, Morton DA. Drug–lactose binding aspects in adhesive mixtures: controlling performance in dry powder inhaler formulations by altering lactose carrier surfaces. Advanced drug delivery reviews. 2012;64(3):275-84.
47. Chew NY, Chan H-K. Influence of particle size, air flow, and inhaler device on the dispersion of mannitol powders as aerosols. Pharmaceutical Research. 1999;16(7):1098-103.
48. Mönckedieck M, Kamplade J, Fakner P, Urbanetz N, Walzel P, Steckel H, et al. Dry powder inhaler performance of spray dried mannitol with tailored surface morphologies as carrier and salbutamol sulphate. International journal of pharmaceutics. 2017;524(1-2):351-63.
49. Hertel N, Birk G, Scherließ R. Performance tuning of particle engineered mannitol in dry powder inhalation formulations. International Journal of Pharmaceutics. 2020;586:119592.
50. Thalberg K, Lindholm D, Axelsson A. Comparison of different flowability tests for powders for inhalation. Powder technology. 2004;146(3):206-13.
51. Rahimpour Y, Kouhsoltani M, Hamishehkar H. Alternative carriers in dry powder inhaler formulations. Drug discovery today. 2014;19(5):618-26.
52. Hersey JA. Ordered mixing: a new concept in powder mixing practice. Powder Technology. 1975;11(1):41-4.
53. Thalberg K, Papathanasiou F, Fransson M, Nicholas M. Controlling the performance of adhesive mixtures for inhalation using mixing energy. International Journal of Pharmaceutics. 2020:120055.
54. Sarangi S, Thalberg K, Frenning G. Numerical Modeling of Collision of Adhesive Units: Stability and mechanical properties during handling. Chemical Engineering Science: X. 2019:100051.
55. Nguyen D, Rasmuson A, Thalberg K, Niklasson Björn I. A breakage and adhesion regime map for the normal impact of loose agglomerates with a spherical target. AIChE Journal. 2015;61(12):4059-68.
56. Nguyen D, Rasmuson A, Björn IN, Thalberg K. Mechanistic time scales in adhesive mixing investigated by dry particle sizing. European Journal of Pharmaceutical Sciences. 2015;69:19-25.
57. De Villiers MM. Description of the kinetics of the deagglomeration of drug particle agglomerates during powder mixing. International Journal of Pharmaceutics. 1997;151(1):1-6.

58. Hertel M, Schwarz E, Kobler M, Hauptstein S, Steckel H, Scherließ R. The influence of high shear mixing on ternary dry powder inhaler formulations. International journal of pharmaceutics. 2017;534(1-2):242-50.
59. Nguyen D, Rasmuson A, Thalberg K, Björn IN. A study of the redistribution of fines between carriers in adhesive particle mixing using image analysis with coloured tracers. Powder Technology. 2016;299:71-6.
60. Faulhammer E, Fink M, Llusa M, Lawrence SM, Biserni S, Calzolari V, et al. Low-dose capsule filling of inhalation products: critical material attributes and process parameters. International journal of pharmaceutics. 2014;473(1):617-26.
61. De Boer A, Dickhoff B, Hagedoorn P, Gjaltema D, Goede J, Lambregts D, et al. A critical evaluation of the relevant parameters for drug redispersion from adhesive mixtures during inhalation. International journal of pharmaceutics. 2005;294(1-2):173-84.
62. Jones MD, Hooton JC, Dawson ML, Ferrie AR, Price R. An investigation into the dispersion mechanisms of ternary dry powder inhaler formulations by the quantification of interparticulate forces. Pharmaceutical research. 2008;25(2):337-48.
63. Thalberg K, Berg E, Fransson M. Modeling dispersion of dry powders for inhalation. The concepts of total fines, cohesive energy and interaction parameters. International journal of pharmaceutics. 2012;427(2):224-33.
64. Adi H, Traini D, Chan H-K, Young PM. The influence of drug morphology on aerosolisation efficiency of dry powder inhaler formulations. Journal of pharmaceutical sciences. 2008;97(7):2780-8.
65. Zhou QT, Armstrong B, Larson I, Stewart PJ, Morton DA. Understanding the influence of powder flowability, fluidization and de-agglomeration characteristics on the aerosolization of pharmaceutical model powders. European Journal of Pharmaceutical Sciences. 2010;40(5):412-21.
66. Dickhoff B, De Boer A, Lambregts D, Frijlink H. The effect of carrier surface and bulk properties on drug particle detachment from crystalline lactose carrier particles during inhalation, as function of carrier payload and mixing time. European Journal of Pharmaceutics and Biopharmaceutics. 2003;56(2):291-302.
67. Kaialy W. On the effects of blending, physicochemical properties, and their interactions on the performance of carrier-based dry powders for inhalation—A review. Advances in colloid and interface science. 2016;235:70-89.
68. Grasmeijer F, Hagedoorn P, Frijlink HW, de Boer AH. Drug content effects on the dispersion performance of adhesive mixtures for inhalation. PloS one. 2013;8(8).
69. Dickhoff B, de Boer A, Lambregts D, Frijlink H. The interaction between carrier rugosity and carrier payload, and its effect on drug particle redispersion from adhesive mixtures during inhalation. European journal of pharmaceutics and biopharmaceutics. 2005;59(1):197-205.
70. Grasmeijer F, Lexmond AJ, van den Noort M, Hagedoorn P, Hickey AJ, Frijlink HW, et al. New mechanisms to explain the effects of added lactose fines on the dispersion performance of adhesive mixtures for inhalation. PloS one. 2014;9(1):e87825.
71. Shalash AO, Molokhia AM, Elsayed MM. Insights into the roles of carrier microstructure in adhesive/carrier-based dry powder inhalation mixtures: carrier porosity and fine particle content. European Journal of Pharmaceutics and Biopharmaceutics. 2015;96:291-303.

72. Elsayed MM, Shalash AO. Modeling the performance of carrier-based dry powder inhalation formulations: Where are we, and how to get there? Journal of Controlled Release. 2018;279:251-61.
73. Renner N, Steckel H, Urbanetz N, Scherließ R. Nano-and Microstructured model carrier surfaces to alter dry powder inhaler performance. International journal of pharmaceutics. 2017;518(1-2):20-8.
74. Crowder TM, Rosati JA, Schroeter JD, Hickey AJ, Martonen TB. Fundamental effects of particle morphology on lung delivery: predictions of Stokes' law and the particular relevance to dry powder inhaler formulation and development. Pharmaceutical research. 2002;19(3):239-45.
75. Jones MD, Santo JG, Yakub B, Dennison M, Master H, Buckton G. The relationship between drug concentration, mixing time, blending order and ternary dry powder inhalation performance. International journal of pharmaceutics. 2010;391(1):137-47.
76. Balducci AG, Steckel H, Guarneri F, Rossi A, Colombo G, Sonvico F, et al. High shear mixing of lactose and salmeterol xinafoate dry powder blends: Biopharmaceutic and aerodynamic performances. Journal of Drug Delivery Science and Technology. 2015;30:443-9.
77. Hertel M, Schwarz E, Littringer EM, Dogru M, Hauptstein S, Steckel H, et al. Influence of blender type on the performance of ternary dry powder inhaler formulations. Drug Delivery to the Lungs. 2016;27:57-60.
78. Zhou QT, Qu L, Gengenbach T, Larson I, Stewart PJ, Morton DA. Effect of surface coating with magnesium stearate via mechanical dry powder coating approach on the aerosol performance of micronized drug powders from dry powder inhalers. Aaps Pharmscitech. 2013;14(1):38-44.
79. Jones MD, Harris H, Hooton JC, Shur J, King GS, Mathoulin CA, et al. An investigation into the relationship between carrier-based dry powder inhalation performance and formulation cohesive–adhesive force balances. European Journal of Pharmaceutics and Biopharmaceutics. 2008;69(2):496-507.
80. Faulhammer E, Wahl V, Zellnitz S, Khinast JG, Paudel A. Carrier-based dry powder inhalation: Impact of carrier modification on capsule filling processability and in vitro aerodynamic performance. International journal of pharmaceutics. 2015;491(1):231-42.
81. Young PM, Wood O, Ooi J, Traini D. The influence of drug loading on formulation structure and aerosol performance in carrier based dry powder inhalers. International journal of pharmaceutics. 2011;416(1):129-35.
82. Donovan MJ, Kim SH, Raman V, Smyth HD. Dry powder inhaler device influence on carrier particle performance. Journal of pharmaceutical sciences. 2012;101(3):1097-107.
83. Clark AR, Weers JG, Dhand R. The Confusing World of Dry Powder Inhalers: It Is All About Inspiratory Pressures, Not Inspiratory Flow Rates. Journal of Aerosol Medicine and Pulmonary Drug Delivery. 2020;33(1):1-11.
84. Hertel M, Schwarz E, Kobler M, Hauptstein S, Steckel H, Scherließ R. Powder flow analysis: A simple method to indicate the ideal amount of lactose fines in dry powder inhaler formulations. International journal of pharmaceutics. 2018;535(1-2):59-67.
85. Abdullah E, Geldart D. The use of bulk density measurements as flowability indicators. Powder Technology. 1999;102(2):151-65.
86. Brown R, Richards JC. Principles of powder mechanics. 1970.

87. Kinnunen H, Hebbink G, Peters H, Shur J, Price R. An investigation into the effect of fine lactose particles on the fluidization behaviour and aerosolization performance of carrier-based dry powder inhaler formulations. AAPS PharmSciTech. 2014;15(4):898-909.
88. Sun Y, Qin L, Liu C, Su J, Zhang X, Yu D, et al. Exploring the influence of drug content on DPI powder properties and potential prediction of pulmonary drug deposition. International Journal of Pharmaceutics. 2020;575:119000.
89. Cordts E, Steckel H. Capabilities and limitations of using powder rheology and permeability to predict dry powder inhaler performance. European Journal of Pharmaceutics and Biopharmaceutics. 2012;82(2):417-23.
90. Alderborn G, Duberg M, Nyström C. Studies on direct compression of tablets X. Measurement of tablet surface area by permeametry. Powder technology. 1985;41(1):49-56.
91. Eriksson M, Nyström C, Alderborn G. The use of air permeametry for the assessment of external surface area and sphericity of pelletized granules. International journal of pharmaceutics. 1993;99(2):197-207.
92. Brunauer S, Emmett PH, Teller E. Adsorption of gases in multimolecular layers. Journal of the American chemical society. 1938;60(2):309-19.
93. Pourghahramani P, Forssberg E. Review of applied particle shape descriptors and produced particle shapes in grinding environments. Part I: Particle shape descriptors. Mineral Processing & Extractive Metall Rev. 2005;26(2):145-66.
94. Tan G, AV Morton D, Larson I. On the methods to measure powder flow. Current pharmaceutical design. 2015;21(40):5751-65.
95. Freeman R. Measuring the flow properties of consolidated, conditioned and aerated powders—a comparative study using a powder rheometer and a rotational shear cell. Powder Technology. 2007;174(1):25-33.
96. Leturia M, Benali M, Lagarde S, Ronga I, Saleh K. Characterization of flow properties of cohesive powders: a comparative study of traditional and new testing methods. Powder Technology. 2014;253:406-23.
97. Schwedes J, Schulze D. Measurement of flow properties of bulk solids. Powder technology. 1990;61(1):59-68.
98. Jenike AW. Storage and flow of solids, bulletin no. 123. Bulletin of the University of Utah. 1964;53(26).
99. Thalberg K, Åslund S, Skogevall M, Andersson P. Dispersibility of lactose fines as compared to API in dry powders for inhalation. International journal of pharmaceutics. 2016;504(1-2):27-38.
100. Council-of-Europe. European Pharmacopoeia. 9.0 ed: European Directorate for the Quality of Medicines & Healthcare; 2017.
101. Wasan D, Kaye B, Wnek W, Davies R, Jackson M. Analysis and evaluation of permeability techniques for characterizing fine particles Part I. Diffusion and flow through porous media. Powder Technology. 1976;14(2):209-28.
102. Sing KS. Assessment of surface area by gas adsorption. Adsorption by Powders and Porous Solids: Principles, Methodology and Applications. 2013:237-63.
103. Jonat S, Hasenzahl S, Drechsler M, Albers P, Wagner K, Schmidt P. Investigation of compacted hydrophilic and hydrophobic colloidal silicon dioxides as glidants for pharmaceutical excipients. Powder technology. 2004;141(1):31-43.
104. Mangal S, Gengenbach T, Millington-Smith D, Armstrong B, Morton DA, Larson I. Relationship between the cohesion of guest particles on the flow behaviour of interactive mixtures. European Journal of Pharmaceutics and Biopharmaceutics. 2016;102:168-77.

105. Krantz M, Zhang H, Zhu J. Characterization of powder flow: Static and dynamic testing. Powder Technology. 2009;194(3):239-45.
106. Clarke MJ, Tobyn MJ, Staniforth JN. The formulation of powder inhalation systems containing a high mass of nedocromil sodium trihydrate. Journal of pharmaceutical sciences. 2001;90(2):213-23.
107. Benassi A, Perazzi I, Bosi R, Cottini C, Bettini R. Quantifying the loading capacity of a carrier-based DPI formulation and its dependence on the blending process. Powder technology. 2019;356:607-17.
108. Venables HJ, Wells J. Powder mixing. Drug development and industrial pharmacy. 2001;27(7):599-612.
109. Pinto JT, Stranzinger S, Kruschitz A, Faulhammer E, Stegemann S, Roblegg E, et al. Insights into the processability and performance of adhesive blends of inhalable jet-milled and spray dried salbutamol sulphate at different drug loads. Journal of Drug Delivery Science and Technology. 2018;48:466-77.
110. Yeung S, Traini D, Tweedie A, Lewis D, Church T, Young PM. Assessing aerosol performance of a dry powder carrier formulation with increasing doses using a novel inhaler. AAPS PharmSciTech. 2019;20(3):94.
111. Yeung S, Traini D, Tweedie A, Lewis D, Church T, Young PM. Limitations of high dose carrier based formulations. International journal of pharmaceutics. 2018;544(1):141-52.
112. Begat P, Price R, Harris H, Morton DA, Staniforth JN. The influence of force control agents on the cohesive-adhesive balance in dry powder inhaler formulations. KONA Powder and Particle Journal. 2005;23:109-21.
113. Begat P, Morton DA, Staniforth JN, Price R. The cohesive-adhesive balances in dry powder inhaler formulations I: Direct quantification by atomic force microscopy. Pharmaceutical research. 2004;21(9):1591-7.
114. Kinnunen H, Hebbink G, Peters H, Huck D, Makein L, Price R. Extrinsic lactose fines improve dry powder inhaler formulation performance of a cohesive batch of budesonide via agglomerate formation and consequential co-deposition. International journal of pharmaceutics. 2015;478(1):53-9.
115. Guchardi R, Frei M, John E, Kaerger J. Influence of fine lactose and magnesium stearate on low dose dry powder inhaler formulations. International journal of pharmaceutics. 2008;348(1-2):10-7.

Acta Universitatis Upsaliensis

Digital Comprehensive Summaries of Uppsala Dissertations from the Faculty of Pharmacy 295

Editor: The Dean of the Faculty of Pharmacy

A doctoral dissertation from the Faculty of Pharmacy, Uppsala University, is usually a summary of a number of papers. A few copies of the complete dissertation are kept at major Swedish research libraries, while the summary alone is distributed internationally through the series Digital Comprehensive Summaries of Uppsala Dissertations from the Faculty of Pharmacy. (Prior to January, 2005, the series was published under the title "Comprehensive Summaries of Uppsala Dissertations from the Faculty of Pharmacy".)

Distribution: publications.uu.se
urn:nbn:se:uu:diva-438081

ACTA
UNIVERSITATIS
UPSALIENSIS
UPPSALA
2021